Geophysical Journal International

*Geophys. J. Int.* (2019) **217,** 1141–1156
Advance Access publication 2019 January 30
GJI Gravity, geodesy and tides

doi: 10.1093/gji/ggz054

# Postglacial gravity change in Fennoscandia—three decades of repeated absolute gravity observations

Per-Anders Olsson,[1] Kristian Breili,[2,3] Vegard Ophaug,[3] Holger Steffen,[1] Mirjam Bilker-Koivula,[4] Emil Nielsen,[5] Tõnis Oja,[6] and Ludger Timmen[7]

[1] *Geodetic Research Division, Lantmäteriet, 801 82 Gavle, Sweden. E-mail: Per-Anders.Olsson@lm.se*
[2] *Geodetic Institute, Norwegian Mapping Authority, 3507 Hønefoss, Norway*
[3] *Faculty of Science and Technology (RealTek), Norwegian University of Life Sciences (NMBU), 1433 Ås, Norway*
[4] *Finnish Geospatial Research Institute, National Land Survey of Finland, 02430 Masala, Finland*
[5] *National Space Institute, Technical University of Denmark (DTU Space), 2800 Kgs. Lyngby, Copenhagen, Denmark*
[6] *Department of Geodesy, Estonian Land Board, 10621 Tallinn, Estonia*
[7] *Institute of Geodesy, Leibniz Universität Hannover (LUH), 30167 Hannover, Germany*

Accepted 2019 January 29. Received 2019 January 23; in original form 2018 September 25

## SUMMARY

For the first time, we present a complete, processed compilation of all repeated absolute gravity (AG) observations in the Fennoscandian postglacial land uplift area and assess their ability to accurately describe the secular gravity change, induced by glacial isostatic adjustment (GIA). The data set spans over more than three decades and consists of 688 separate observations at 59 stations. Ten different organizations have contributed with measurements using 14 different instruments. The work was coordinated by the Nordic Geodetic Commission (NKG). Representatives from each country collected and processed data from their country, respectively, and all data were then merged to one data set. Instrumental biases are considered and presented in terms of results from international comparisons of absolute gravimeters. From this data set, gravity rates of change ($\dot{g}$) are estimated for all stations with more than two observations and a timespan larger than 2 yr. The observed rates are compared to predicted rates from a global GIA model as well as the state of the art semi-empirical land uplift model for Fennoscandia, NKG2016LU. Linear relations between observed $\dot{g}$ and the land uplift, $\dot{h}$ (NKG2016LU) are estimated from the AG observations by means of weighted least squares adjustment as well as weighted orthogonal distance regression. The empirical relations are not significantly different from the modelled, geophysical relation $\dot{g} = 0.03 - 0.163(\pm 0.016)\dot{h}$. We also present a $\dot{g}$-model for the whole Fennoscandian land uplift region. At many stations, the observational estimates of $\dot{g}$ still suffer from few observations and/or unmodelled environmental effects (e.g. local hydrology). We therefore argue that, at present, the best predictions of GIA-induced gravity rate of change in Fennoscandia are achieved by means of the NKG2016LU land uplift model, together with the geophysical relation between $\dot{g}$ and $\dot{h}$.

**Key words:** Geodetic instrumentation; Reference systems; Time variable gravity; Europe; Dynamics of lithosphere and mantle.

## 1 INTRODUCTION

Glacial isostatic adjustment (GIA) is the response of the Earth to changing loads on its surface due to build-up and ablation of ice sheets and glaciers. The response includes changes in shape (deformation), gravity potential, stress and rotation of the Earth (Wu & Peltier 1982). The effects of GIA that are presently observed result from several glaciations with ice sheets covering large parts of, for example, North America, Northern Europe and Patagonia.

The last glaciation peaked about 22 000 yr ago in Fennoscandia (Lambeck *et al.* 2010). Although the ice vanished about 10 000 yr ago (Lambeck *et al.* 2010), the Earth is still readjusting due to the viscoelastic nature of the mantle, which leads to time-delayed processes. In Fennoscandia, this is visible in the ongoing surface uplift that peaks at about 1 cm yr$^{-1}$ near the Swedish coast to the Gulf of Bothnia (Steffen & Wu 2011; Fig. 1).

The GIA process in Fennoscandia is well known and extensively studied. Ekman (1991) describes the early history of research within

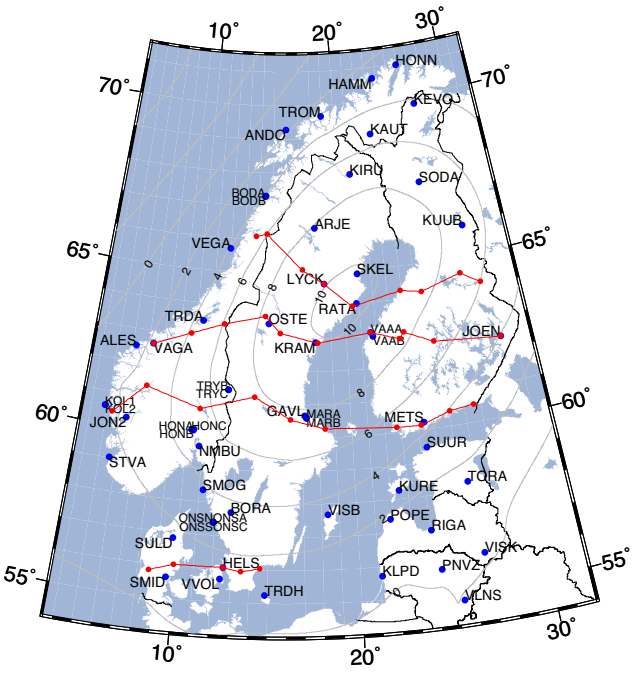


**Figure 1.** Stations with repeated gravity observations in Fennoscandia. Blue dots represent absolute gravity stations and red dots (and lines) the Fennoscandian land uplift gravity lines with relative observations. Isolines show the vertical displacement rate according to the semi-empirical land uplift model NKG2016LU_abs (mm $yr^{-1}$).

this field and Steffen & Wu (2011) review modern observational and modelling efforts in this region.

One important observable of GIA, but less used and investigated compared to deformation, is the secular gravity change. Redistribution of masses within the Earth as well as on the surface cause changes in the gravity field. Also the vertical land motion/uplift itself induces changes in gravity on the surface of the Earth. Knowledge about this GIA-induced rate of change of gravity, $\dot{g}$, is important in many aspects, for example

(1) for reduction of terrestrial gravity observations to a certain epoch,
(2) as ground truth for satellite gravity missions (e.g. Steffen *et al.* 2009; Müller *et al.* 2012), and
(3) for constraining and tuning GIA models (e.g. Steffen *et al.* 2014; Van Camp *et al.* 2017).

Several models of the GIA-induced vertical displacement rate have been published for Fennoscandia (e.g. Ekman 1996; Lambeck *et al.* 1998; Milne *et al.* 2004; Ågren & Svensson 2007; Lidberg *et al.* 2010). Although several observational $\dot{g}$-results exist (see Table 1), no $\dot{g}$-model for Fennoscandia has been published so far. This is primarily because terrestrial gravity measurements are time consuming and need on-site manpower. Absolute gravity (AG) observations are consequently more expensive than most other geodetic observations. In addition, combination of gravity measurements is challenging due to sensor-affecting incidents and local gravity effects that may mask the secular trend due to GIA.

The first systematic observations of the GIA-induced gravity change were repeated *relative* gravity observations along the so-called Fennoscandian land uplift gravity lines. They consist of four east-west high precision relative gravity profiles, approximately following the latitudes 65°, 63°, 61° and 56° (see Fig. 1). Measurements along the Finnish part of the 63° line started in 1966 followed by the rest of the lines from the mid-1970s (Kiviniemi 1974; Ekman & Mäkinen 1996; Mäkinen *et al.* 2005). The work with the Fennoscandian land uplift gravity lines was initiated and coordinated by the Nordic Geodetic Commission (NKG).

From the late 1980s the relative gravity observations along the uplift lines have been complemented and gradually succeeded by repeated *AG* observations. In 1988, the Finnish Geodetic Institute (FGI) started this work using a free-fall absolute gravimeter JILAg-type (Torge *et al.* 1987), JILAg#5. This gravimeter was mainly used in Finland but also at some stations in the other Scandinavian and especially the Baltic countries. During the 1990s, the JILAg measurements were complemented by observations with its successor, the FG5 (Niebauer *et al.* 1995). These first FG5 campaigns were performed by the National Oceanic and Atmospheric Administration (NOAA), USA, in 1993 and 1995. Further FG5 campaigns were conducted by the Bundesamt für Kartographie und Geodäsie (BKG) in 1993, 1995, 1998 and 2003 on 15 stations distributed in the uplift area. In 2003–2008 comprehensive campaigning was carried out with an FG5 instrument by the Leibniz Universität Hannover (LUH), Germany. During that time also the FGI, the Norwegian University of Life Sciences (NMBU) and Lantmäteriet (the Swedish mapping, cadastral and land registration authority) invested in FG5 gravimeters and started with repeated AG observations. In 2008 the Technical University of Denmark (DTU) started making repeated measurements with their A10 absolute gravimeter (Micro-g LaCoste 2008). Today there are 688 AG observations on 59 stations in the region (Fig. 1), most of them co-located with Global Navigation Satellite Systems (GNSS) reference stations. Two of the stations, Metsähovi (since 1994; Virtanen 2006) and Onsala (since 2008), also house superconducting gravimeters (SG). As in the case of the land uplift lines, the work with absolute observations was and is coordinated by the NKG.

Only parts of the Fennoscandian repeated AG observations have hitherto been published. Gitlein (2009) published the results from the BKG, NOAA and LUH campaigns in 1993–2008 with focus on the LUH data. Ophaug *et al.* (2016) published all FG5 data on the Norwegian stations. Selected observations have been included in special studies, for example, to address the $\dot{g}/\dot{h}$ ratio (Pettersen 2011). Table 1 gives an overview of publications addressing different parts of the whole data set. This includes some unpublished reports and poster presentations since they, in the absence of better references, sometimes have been cited in the literature.

Besides Fennoscandia, GIA-induced surface deformation and gravity changes can also be observed in North America. Compared to Fennoscandia, both the signal strength and the geographical extent are larger. AG time-series from North America was analysed by, for example, Larson & van Dam (2000) and Lambert *et al.* (2001, 2006, 2013a,b). A map of gravity rate of change in North America, but mainly based on relative gravity measurements, was published by Pagiatakis & Salib (2003). In their study, they readjusted the primary Canadian Gravity Standardization Network using relative gravity measurements spanning over 40 yr. The gravity rate of change was introduced as an unknown in the observation equation and AG measurements were used as weighted constraints in the (least squares) adjustment.

The relation between $\dot{g}$ and the vertical displacement rate of the crust, $\dot{h}$, is also an important observable since it

(1) is affected by both the vertical movement itself as well as by mass changes beneath the surface and therefore contains information on the underlying geophysics and geodynamics (e.g. Ekman & Mäkinen 1996; de Linage *et al.* 2009),

**Table 1.** Overview of important publications and reports on repeated AG observations in Fennoscandia.

| Reference | Data set | Comment |
|---|---|---|
| Roland (1998) | 1991–1995. Observations at 23 stations in Finland, Norway and Sweden | Technical report NMA (in Norwegian) |
| Engfeldt *et al.* (2006) | 2003–2005. $\dot{g}$ at 14 stations in Finland, Norway and Sweden. Only FG5 | Poster |
| Mäkinen *et al.* (2006) | 1976–2006. $\dot{g}$ at Finnish stations | Poster |
| Bilker-Koivula *et al.* (2008) | 1976–2007. Observations at six Finnish stations | |
| Gitlein (2009) | 1993–2008. Observations at 37 stations in the Scandinavian and Baltic countries. Only NOAA, BKG and LUH | PhD thesis |
| Steffen *et al.* (2009) | 2004–2007. Six stations. Only LUH | Ground truth for GRACE |
| Breili *et al.* (2010) | $g$ at Norwegian stations from observations with FG5#226 | |
| Mäkinen *et al.* (2010) | 1988–2009. $\dot{g}$ at 23 stations in the Scandinavian and Baltic countries | Poster |
| Pettersen (2011) | From Engfeldt *et al.* (2006) | Address the $\dot{g}/\dot{h}$-ratio |
| Timmen *et al.* (2012) | 2004–2008. From Gitlein (2009). Only LUH | $\dot{g}/\dot{h}$=0.163 |
| Müller *et al.* (2012) | Same as Timmen *et al.* (2012) | Ground truth for GRACE |
| Nordman *et al.* (2014) | Timmen *et al.* (2012), Pettersen (2011), and Breili *et al.* (2010) | Compare $\dot{g}$ and $\dot{h}$ from different sources |
| Timmen *et al.* (2015) | 2003–2014. Only Onsala. Only FG5#220 and FG5#233 | Evaluate $\dot{g}$ |
| Ophaug *et al.* (2016) | 1993–2014. Only Norwegian stations | |

(2) is used for evaluation of global Terrestrial Reference Frames (e.g. Mazzotti *et al.* 2011; Collilieux *et al.* 2014) and

(3) is used for separating the GIA signal from present-day ice melting signals in Greenland and Antarctica (e.g. Wahr *et al.* 1995; van Dam *et al.* 2017).

In addition, a trustworthy relation between $\dot{g}$ and $\dot{h}$ also allows us to make transformations between, and combine, the two observables.

As mentioned, in regions like Antarctica and Greenland, the ratio between $\dot{g}$ and $\dot{h}$ has been used for separating the present-day ice-mass change signal from the GIA signal, the latter induced by historical ice mass variations (Wahr *et al.* 1995; James & Ivins 1998; Fang & Hager 2001; Purcell *et al.* 2011; Memin *et al.* 2012). From an analytical study with a GIA model for Greenland and Antarctica, Wahr *et al.* (1995) found the viscous part of the ratio to be $\sim -0.154$ μGal mm$^{-1}$. Using the ice model ICE-3G, James & Ivins (1998) predicted $\dot{g}$ and $\dot{h}$ for Antarctica, and found their ratio to be $\sim -0.16$ μGal mm$^{-1}$. These predictions are based on modelling and are difficult to verify by observations, because gravity change due to present-day ice mass variation is superimposed by the viscous gravity signal.

In North America and Fennoscandia the situation is different. Here, the signal is strongly dominated by the past GIA signal and the ice-free conditions make it possible to conduct repeated measurements of both gravity and height changes. Table 2 summarizes published ratios based on observations in these regions.

Olsson *et al.* (2015) investigated the geophysical relation between $\dot{g}$ and $\dot{h}$ in previously glaciated areas (like Fennoscandia and Laurentia) using a GIA model, similar to the one described in Section 2.5, and found that

(1) their ratio varies in the spectral domain and is smaller (less negative) in the lower part of the spectrum, implying that for a region where the GIA signal is smooth and has a large geographical extent (Laurentia) the ratio is expected to be smaller than for a region where higher degrees of the spectrum dominate the signal (Fennoscandia),

(2) the borderline between the uplift area and the forebulge area (zero line) for $\dot{g}$ and $\dot{h}$ does not exactly coincide, which affects their ratio especially where the signal is small,

(3) within Fennoscandia the ratio varies laterally in such a way that for practical applications these variations can be neglected,

(4) local effects, such as direct attraction and short wavelength elastic deformation from present-day GIA-induced sea level variations do not significantly affect the ratio other than in extreme cases (when the station in question is located very close to and high above the sea).

These conclusions imply that for Fennoscandia it is a reasonable assumption to estimate a single linear relation between $\dot{g}$ and $\dot{h}$ for the entire region.

For the first time we present estimated gravity rates of change based on all repeated gravity observations, spanning over three decades, in the Fennoscandian land uplift area. All observations are provided and described in detail. Estimated $\dot{g}$ values are assessed by the geophysical relation between $\dot{g}$ and $\dot{h}$, found from GIA-modelling, and the uncertainties in these relations are discussed. We also suggest a $\dot{g}$ model covering the whole area, based on the state of the art land uplift model and the geophysical relation between $\dot{g}$ and $\dot{h}$.

In Section 2, we describe the AG data set, how data from different sources have been processed and merged, known error sources, and uncertainty estimates. We also introduce land uplift data sets and a geophysical GIA model for comparison to our observational gravity rate of change. In Section 3, we estimate observational values of $\dot{g}$ and compare it with a semi-empirical land uplift model as well as a pure GIA model. The relation between $\dot{g}$ and $\dot{h}$ is estimated and studied in Section 4 and it is further used for constructing a $\dot{g}$-model, covering the whole area. This is followed by a discussion of the results and a summary of conclusions. Detailed information about the stations and all observations are provided as Supporting Information (Tables S2 and S4).

## 2 DATA AND MODELS

### 2.1 The AG stations

We have used data from 59 stations in the region where repeated AG observations have been conducted (Fig. 1 and Table S2). Steffen *et al.* (2012) studied optimal locations for AG observations and concluded that, except for the northwestern part of Russia, these

**Table 2.** Published observations of $\dot{g}/\dot{h}$ in previously glaciated areas (from Olsson *et al.* 2015).

| Area | $\dot{g}/\dot{h}$ ($\mu$Gal mm$^{-1}$) | Note | References |
|---|---|---|---|
| Fennoscandia | $-0.204 \pm 0.058$ | Relative gravity observations every 5th yr; time span ~27 yr. $\dot{h}$ from mareographs and levelling | Ekman & Mäkinen (1996) |
| Fennoscandia | $-0.16 \pm 0.05$ to $-0.18 \pm 0.06$ | Ekman & Mäkinen (1996) revisited, this time with more observations of $\dot{g}$ as well as $\dot{h}$ (including GNSS) | Mäkinen *et al.* (2005) |
| Fennoscandia | $-0.163 \pm 0.02$ | Four years of annual AG-observations on eight stations. $\dot{h}$ from GNSS (Lidberg *et al.* 2007). For the different stations, the ratios vary between $-0.114 \pm 0.031$ and $-0.232 \pm 0.059$ $\mu$Gal mm$^{-1}$ | Timmen *et al.* (2012) |
| Fennoscandia | $-0.17$ to $-0.22$ | 13 stations with repeated AG observations compared to vertical rates derived from tide-gauge data and GNSS data | Pettersen (2011) |
| Laurentia | $\sim -0.154$ | Four stations of co-located GNSS and AG. Total time span 6 yr. The ratio $-0.154$ $\mu$Gal mm$^{-1}$ is within the error bars of these observations | Larson & van Dam (2000) |
| Laurentia | $-0.18 \pm 0.03$ | Four stations of co-located GNSS and AG. Three of the stations are the same as in Larson & van Dam (2000) | Lambert *et al.* (2006) |
| Laurentia | $-0.17 \pm 0.01$ | Eight AG stations whereof six are co-located with GNSS including the four stations in Lambert *et al.* (2006). Time spans 7–21 yr | Mazzotti *et al.* (2011) |
| Alaska | $-0.21 \pm 0.09$ and $-0.18 \pm 0.05$ | The viscous part of the ratio in an area affected by present-day ice mass change. Different ratios depending on how the present-day signal is corrected for | Sato *et al.* (2012) |

stations form a complete and adequate network for providing constraints for the study of GIA parameters.

Most of the stations are co-located with permanent GNSS reference stations in the so-called BIFROST (Baseline Inference for Fennoscandian Rebound Observations, Sea level and Tectonics) network (see e.g. Johansson *et al.* 2002; Lidberg *et al.* 2010). Many of these stations have GNSS time-series spanning more than 20 yr. The AG stations typically consist of a concrete pillar mounted directly on solid bedrock, housed in the same building as the GNSS station (Fig. 2). Some of the stations (e.g. Metsähovi, Mårtsbo, Onsala and Trysil) have two or more pillars and are therefore suitable for comparisons of instruments by means of simultaneous observations. Some stations are not dedicated AG stations but rather housed in public, stable buildings.

Metsähovi (MET) and Onsala (ONS) are geodetic fundamental stations in the sense that they host instrumentation for a large variety of observational techniques like AG, superconducting gravity, very long baseline interferometry, satellite laser ranging (MET), tide gauge (ONS) and monitoring of local hydrology.

In addition to the stations discussed above, some hundred other AG stations have also been observed with absolute gravimeters (typically A10 gravimeters). These are more simple stations like a benchmark mounted in a rock, stairs or similar. The purpose of these observations was not to study GIA or other geophysical processes and phenomena but rather to serve as datum points for national gravity reference systems. These stations and observations are therefore not treated here.

### 2.2 The AG observations

During the time period 1988–2015, 688 repeated AG observations were conducted at the stations described above. *One observation* is here understood to be the mean of a large number of free fall experiments (*drops*). The drops are normally executed during a time period of ~12–48 hr and grouped in *sets* of ~50–100 drops. If there was more than one consecutive set-up of the instrument (e.g. with different orientations) at one visit of the station, then the results of the different set-ups are merged to one observation.

Many different organizations have contributed with observations (Table 3). Each organization initially processed their own data. One representative for each country (Table S1) then collected, and in some cases reprocessed, all data from stations in his/her country, respectively. Data from all participating countries have then been merged into one database (Table S4).

The bulk of the observations was collected using FG5 gravimeters (Niebauer *et al.* 1995). These data were processed using the 'g' software (Micro-g LaCoste 2012) with final International Earth Rotation and Reference System Service (IERS) polar coordinates, calibrated rubidium frequencies, and standard modelling of gravitational effects due to earth tides, ocean loading and varying atmospheric pressure, as implemented in the 'g' software [for details concerning e.g. ocean tide loading (OTL) models, see Supporting Information]. There have been attempts to perform a refined modelling of the gravitational effect due to ocean loading, non-tidal ocean loading and global hydrology (Ophaug *et al.* 2016), as well as the atmosphere (Gitlein 2009; Ophaug *et al.* 2016). The general conclusions of these studies are that refined modelling does not give any significant improvement with respect to the gravity trends on average. In addition, the lack of corrections for local hydrology, which could dominate the gravity rate at a specific site, is identified as an important issue for further research (see e.g. Van Camp *et al.* 2016b). Thus, until the refined modelling improves and the effect of local hydrology can be embedded, we stick with the standard processing scheme in this work.

Apart from FG5 also IMGC (Germak *et al.* 2006), GABL (Arnautov *et al.* 1983), JILAg (Niebauer *et al.* 1986) and A10 (Micro-g LaCoste 2008) absolute gravimeters were used (see Table 3).

All data are presented in the zero tide system. Some of the first observations (e.g. IMGC from 1976) were originally in the mean tide system but have been reprocessed to the zero tide system (Haller & Ekman 1988), following the IAG resolution from 1983 (IAG 1984).

Details about the data and data processing are given in the Supporting Information.

### 2.3 Instrumental biases

AG observations are in general sensitive to instrumental biases (or offsets). In order to detect such biases the International Bureau of Weights and Measures (BIPM) organized international comparisons of absolute gravimeters on a regular basis between 1981 and


**Figure 2.** Example of a typical AG station: Arjeplog, Sweden (ARJE).

**Table 3.** Absolute gravimeters used for collecting the data in Denmark, Estonia, Latvia, Lithuania, Finland, Norway and Sweden.

| Organization | Instrument | Number of observations | Timespan (yr) |
|---|---|---|---|
| Instituto di Metrologia G. Colonnetti (IMGC), Turin, Italy | IMGC | 2 | 1976 |
| Russian Academy of Science (AN SSSR) | GABL | 2 | 1980 |
| Finnish Geodetic Institute (FGI), Masala, Finland | JILAg#5 | 116 | 1988–2002 |
| | FG5#221[a] | 172 | 2003–2013 |
| National Oceanic and Atmospheric Administration (NOAA), Silver Spring, Maryland, USA | FG5#102 | 10 | 1993 |
| | FG5#111 | 16 | 1995–1997 |
| Bundesamt für Kartographie und Geodäsie (BKG), Frankfurt/Main, Germany | FG5#101 | 15 | 1993–2006 |
| | FG5#301 | 11 | 2003 |
| National Geospatial-Intelligence Agency (NGA), St. Louis, USA | FG5#107 | 1 | 1996 |
| Leibniz Universität Hannover (LUH), Germany | FG5#220[b] | 92 | 2003–2015 |
| Norwegian University of Life Sciences (NMBU), Ås, Norway | FG5#226 | 99 | 2004–2014 |
| Lantmäteriet (LM), Gävle, Sweden | FG5#233 | 138 | 2006–2015 |
| Technical University of Denmark (DTU), Lyngby, Denmark | A10#19 | 11 | 2008–2015 |
| Instytut Geodezji i Kartografii, Warszawa, Poland | A10#20 | 3 | 2011 |

[a]Upgraded to FG5X#221 in 2013.3.
[b]Upgraded to FG5X#220 in 2012.5.

2009 in Sèvres, France. Since 2003 these have been complemented with regional comparisons and after 2009 CCM comparisons (Consultative Committee for Mass and Related Quantities) were held at different locations, keeping the 4 yr cycle (Table 4). For each comparison a Comparison Reference Value (CRV) is determined by the participating instruments and individual instrumental biases relative to the CRV are determined for each instrument. Table 5 summarizes the results for the instruments relevant for this work. The methods for determining CRVs, biases and especially uncertainties have varied through the years. In later years the officially given uncertainties include a systematic component for each instrument which is, in general, not the case for the results of the early comparisons. In order to make the numbers in Table 5 comparable to each other, we have chosen to provide the $2\sigma$ uncertainty from the adjustment/estimation of the instrumental biases. Also, since the sign of the reported offset/DoE (degree of equivalence) has changed over the years all values have been converted to DoE (Instrument#XXX-CRV).

Table 5 shows that the participating instruments normally agree with the CRV within the uncertainty limits. In a few cases the estimated bias is larger than two times the standard uncertainty and in only two cases (JILAg#5 2001 and FG5#220 2015) the bias is larger than three times the standard uncertainty. As mentioned before, the uncertainties given in Table 5 are taken as two times the standard uncertainty of the estimated biases (from the adjustment), which is how the uncertainties for the first comparisons were reported. The modern way of reporting expanded total uncertainty was not reproducible for these old results. In order to make all results in Table 5 comparable we had to choose this way of giving the uncertainty. From 2009 the officially published uncertainties are found directly from the expanded total measurement uncertainty reported for each instrument combined with the uncertainty of the estimated CRV. This method results in larger uncertainty estimates than those in Table 5, and based on these, none of the instruments in Table 5 was reported to have significant biases compared to the CRV.

Our study includes data from one JILAg instrument (#5). Table 5 indicates that it might have been biased and that the bias might have changed but these results are not significant. Other institutions have also reported on biases for their JILAg instruments. For JILAg#3 of the Hannover group (LUH), an obtained discrepancy to the FG5#220 (LUH) of +9.0 μGal indicates a significant long-term offset between the measuring levels of the two gravimeters (Timmen *et al.* 2011). Similar discrepancies have also been reported by Torge *et al.* (1999) when comparing measurements from FG5#101 (BKG) and JILAg#3 performed in the years 1994–1997. These comparisons showed a discrepancy varying between +8.1 and +9.4 μGal. It is interesting that the same long-term bias of +9 Gal was also determined for the JILAg#6 gravimeter (see Pálinkáš

**Table 4.** Overview of official international (ICAG), European (ECAG) and regional (EURAMET) Comparisons of absolute gravimeters, held in Sèvres (France) until the year 2015, Walferdange and Belval (Luxembourg). The standard deviations ($1\sigma$) of all participating instruments' degrees of equivalences (DoEs) are also given for each campaign.

| Comparison | Location | Approximate epoch | $\sigma$ of DoEs ($\mu$Gal) | Reference |
|---|---|---|---|---|
| ICAG 81-82 | Sèvres | 1982.0 | ∼8 | Boulanger *et al.* (1983) |
| ICAG 1985 | Sèvres | 1985.5 | 4.4 | Boulanger *et al.* (1986) |
| ICAG 1989 | Sèvres | 1989.5 | 7.6 | Boulanger *et al.* (1991) |
| ICAG 1994 | Sèvres | 1994.4 | 3.3 | Marson *et al.* (1995) |
| ICAG 1997 | Sèvres | 1997.9 | 2.8 | Robertsson *et al.* (2001) |
| ICAG 2001 | Sèvres | 2001.6 | 5.5 | Vitushkin *et al.* (2002) |
| ECAG 2003 | Walferdange | 2003.8 | 1.9 | Francis & van Dam (2006) |
| ICAG 2005 | Sèvres | 2005.7 | 3.7 | Jiang *et al.* (2011) |
| ECAG 2007 | Walferdange | 2007.9 | 2.1 | Francis *et al.* (2010) |
| ICAG 2009 | Sèvres | 2009.8 | 4.2 | Jiang *et al.* (2012) |
| ECAG 2011 | Walferdange | 2011.9 | 3.1 | Francis *et al.* (2013) |
| ICAG 2013 | Walferdange | 2013.9 | 3.8 | Francis *et al.* (2015) |
| EURAMET 2015 | Belval | 2015.8 | 5.1 | Pálinkáš *et al.* (2017) |

**Table 5.** Official results from the international comparisons in Table 4. The numbers correspond to the degree of equivalence (DoE), that is the estimated bias of each instrument, compared to comparison reference values, and the associated expanded uncertainty (∼95% confidence level ($2\,\sigma$)). Only results relevant for this work are presented.

| | IMGC | GABL | JILAg#5 | FG5#101 | FG5#102 | FG5#111 | FG5#107 |
|---|---|---|---|---|---|---|---|
| ICAG 81-82 | −6 | 7 | | | | | |
| ICAG 1985 | | | | | | | |
| ICAG 1989 | | | −8.1 ± 6.6 | | | | |
| ICAG 1994 | | | −3.9 ± 8 | −0.5 ± 6.4 | −2.1 ± 6 | | 1.7 ± 6 |
| ICAG 1997 | | | 0.5 ± 7.2 | −2.7 | | | 2.5 ± 6.0 |
| ICAG 2001 | | | 5.7 ± 3.2 | 2.9 ± 8.0 | | | |
| ECAG 2003 | | | | | | | |
| ICAG 2005 | | | | −2.5 ± 3.0 | | | |
| ECAG 2007 | | | | 2.2 ± 1.8 | | | |
| | FG5#301 | FG5#220 | FG5#221 | FG5#226 | FG5#233 | A10#19 | A10#20 |
| ICAG 2001 | −4.5 ± 5.6 | | | | | | |
| ECAG 2003 | −1.3 ± 2.0 | −1.8 ± 2.8 | 0.9 ± 3.8 | | | | |
| ICAG 2005 | | | −0.5 ± 3.6 | | | | |
| ECAG 2007 | | 2.5 ± 2.2 | 0.1 ± 2.2 | −3.4 ± 2.4 | 1.0 ± 1.8 | | |
| ICAG 2009 | | 1.7 ± 2.8 | 1.6 ± 3.2 | | 1.0 ± 2.8 | | 5.0 ± 12.2 |
| ECAG 2011 | | 1.8 ± 3.2 | 0.0 ± 3.6 | | 4.7 ± 3.3 | | −5.1 ± 11.7 |
| ICAG 2013 | | 2.3 ± 3.1[1] | 1.5 ± 3.3[a] | | 2.2 ± 3.4 | | −4.6 ± 6.5 |
| EURAMET 2015 | | 5.2 ± 2.9[1] | −2.1 ± 3.3[1] | | 2.5 ± 3.4 | | −5.3 ± 7.5 |

[a]Upgraded to FG5X.

*et al.* 2012). For the Canadian gravimeter JILAg#2 a systematic offset of +4.1 $\mu$Gal has been found in Liard *et al.* (2003). Some hints are given in Wilmes *et al.* (2003) that similar offsets may exist in other JILA gravimeters with respect to FG5 meters. Besides these long-term biases, varying biases valid for shorter periods may exists for gravimeters and depend on the experts who re-adjust the instruments from time to time.

One major disadvantage of the JILAg design compared with the FG5 instruments is the high sensitivity of JILAg meters to floor tilts occurring during each drop which is triggered by the dropping mechanism similar in all drops of a measuring set. Because the interferometer design is not following the Abbe rule like it is realized in the FG5 instruments (reference and test prism in one vertical line), tilt coupling errors of some microgal could occur at locations with weak floor conditions. That introduces a systematic error in the station determination by the gravimeter and can only be detected by a new set-up of the meter with another orientation. For FG5 gravimeters, the effect has been minimized, see Niebauer *et al.* (1995).

By assessing local comparisons between some of the instruments relevant for this study also Pettersen *et al.* (2010) conclude that data from these instruments reveal no systematic biases, but occasional shifts from 1 yr to another are noted. This was also found by Olsson *et al.* (2016). They showed that time-series from the FG5#233 gravimeter indicated a jump in 2010. The jump occurred during a service of the instrument by the manufacturer, but no real explanation has been found, yet. The effects of that jump could be reduced by introducing a small correction based on the results from the international comparisons.

Based on the results above, data from FG5#233 have been corrected for the suspected jump in this study (see further Section 3) but no other biases between instruments have been considered.

### 2.4 The NKG2016LU land uplift model

NKG2016LU is a successor of the empirical land uplift model NKG2005LU, which has been the official standard model for geodetic land uplift applications in the Nordic countries for the last decade.

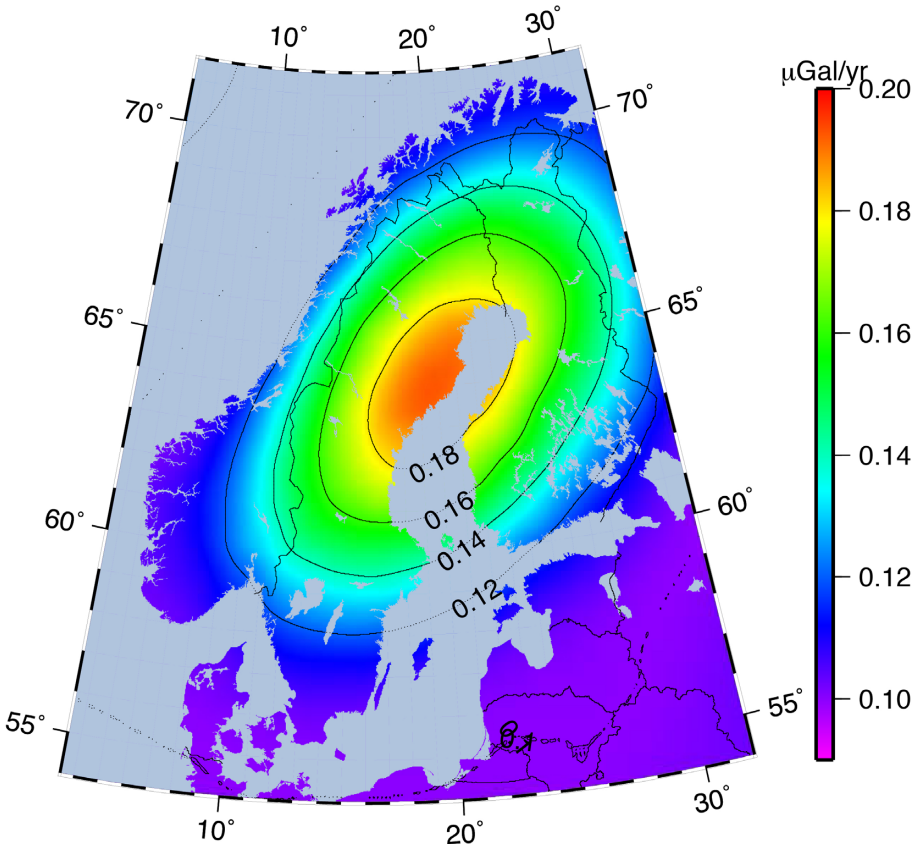


**Figure 3.** Uncertainty of $\dot{g}$ predicted using the land uplift model NKG2016LU_abs together with a geophysical relation between $\dot{g}$ and $\dot{h}$.

NKG2005LU was released by the NKG Working Group for Height Determination in 2006. Empirical here means that it heavily relies on geodetic observations such as repeated levelling and time-series from tide gauges and GNSS stations. The different types of observations are combined by means of least squares collocation. For interpolation (and extrapolation) between the observation points, a geophysical GIA model by Lambeck *et al.* (1998) was used. For a thorough description of NKG2005LU, see Ågren & Svensson (2007) and Vestøl (2007).

In 2016, the NKG Working Group on Geoid and Height Systems released the land uplift model NKG2016LU, which is now called semi-empirical in order to emphasize that it, in addition to observations, also includes a GIA modelling component. Notable differences to NKG2005LU include

(1) longer GNSS time-series. Vertical velocities from the BIFROST 2015/16 calculation, processed in GAMIT/GLOBK and finalized in 2016 March 1. This is an updated version of Kierulf *et al.* (2014).

(2) omission of tide gauge data. Spatial and especially temporal variations in the rate of change of mean sea level (e.g. accelerating sea level rise during the last decades) prompted the decision not to include tide gauge data in NKG2016LU.

(3) more thorough GIA modelling, better adapted to geodetic observations in Fennoscandia (Steffen *et al.* 2016).

NKG2016LU comes in two versions, NKG2016LU_lev and NKG2016LU_abs. NKG2016LU_lev is the land uplift as measured with repeated levelling, that is relative to the geoid. NKG2016LU_abs (see Fig. 1) is the absolute land uplift in ITRF2008 as observed by GNSS. In the observation points, the mean difference between the BIFROST GNSS solution and the final NKG2016LU_abs model is $0.02 \pm 0.42$ ($1\sigma$) mm yr$^{-1}$, which corresponds to $\sim -0.003 \pm 0.07$ ($1\sigma$) $\mu$Gal yr$^{-1}$ (see below). As NKG2016LU is given in the same reference frame as the BIFROST GNSS solution, but also includes levelling data, and gives a trustworthy interpolation between the observation points (and thus a value for all gravity points and any other point), we take it rather than the GNSS solution itself as a reference model.

For conversion of the NKG2016LU_abs land uplift to gravity rate of change we use the factor $C = -0.163$ μGal mm from$^{-1}$ the modelled linear relation

$$\dot{g} = 0.03 - 0.163\dot{h}, \tag{1}$$

found by Olsson *et al.* (2015), valid for 1-D geophysical GIA models (normal mode approach) in Fennoscandia. The uncertainty of the factor has been estimated to $u(C) \sim \pm 0.016$ μGal mm$^{-1}$ (Ophaug *et al.* 2016).

Assuming an internal uncertainty of 0.2 mm yr$^{-1}$ in NKG2016LU_abs (Jonas Ågren, personal communication, 2016) and uncertainties in the drift of the origin relative to the Earth's centre of mass and in the scale of ITRF2008 of 0.5 and 0.3 mm yr$^{-1}$, respectively (Collilieux *et al.* 2014), we estimate the total uncertainty of NKG2016LU_abs to $u(\dot{h}) \sim 0.6164$ mm yr$^{-1}$ by error propagation. Then the uncertainty of the predicted gravity change is $u(\dot{g}_{\mathrm{LU}}) = \sqrt{u(C)^2\dot{h}^2 + u(\dot{h})^2C^2} = \sqrt{0.016^2\dot{h}^2 + 0.010}$ μGal yr$^{-1}$ where $\dot{g}_{\mathrm{LU}} = C \cdot \dot{h}_{NKG2016LU\_abs}$. In Fennoscandia $0.1 \leq u(\dot{g}_{\mathrm{LU}}) < 0.2$ (μGal yr$^{-1}$) (see Fig. 3).

**Table 6.** Absolute land uplift rate, $\dot{h}$ (mm yr$^{-1}$) and gravity rate of change, $\dot{g}$ ($\mu$Gal yr$^{-1}$). Subscript *GNSS* referes to the BIFROST 2015/16 solution, *GIA* to the geophysical GIA model, *LU* means -0.163·NKG2016LU_abs and *I* and *II* are estimates based on the corresponding data sets (see text). $\bar{\varepsilon}$ are the standardized residuals from the estimations of $\dot{g}/\dot{h}$ trend lines (eq. 4). The last two columns show the total number of AG observations (corresponding to Dataset I) at each station and their time span [years].

| Stn | $\dot{h}_{LU}$ | $\dot{h}_{GNSS}$ | $\dot{g}_{GIA}$ | $\dot{g}_{LU}$ | $\dot{g}_{I}$ | $\bar{\varepsilon}_{I}$ | $\dot{g}_{II}$ | $\bar{\varepsilon}_{II}$ | $n_{obs}$ | $\Delta T$ |
|---|---|---|---|---|---|---|---|---|---|---|
| ALES | 1.63 | 1.73 | −0.05 | −0.27 ± 0.10 | −0.29 ± 0.48 | −0.2 | −0.29 ± 0.36 | −0.3 | 5 | 7.0 |
| ANDO | 1.69 | 1.26 | 0.09 | −0.28 ± 0.10 | −1.09 ± 0.55 | −1.6 | −1.09 ± 0.41 | −2.2 | 5 | 6.0 |
| ARJE | 8.15 | 7.97 | −1.02 | −1.33 ± 0.16 | −0.74 ± 0.31 | 1.9 | −1.09 ± 0.23 | 1.1 | 11 | 10.0 |
| BODA | 3.94 | | −0.35 | −0.64 ± 0.12 | −2.23 ± 0.72 | −2.3 | | | 4 | 5.1 |
| BODB | 3.96 | 3.88 | −0.35 | −0.65 ± 0.12 | −1.06 ± 0.83 | −0.5 | | | 4 | 4.0 |
| BORA | 3.52 | 3.58 | −0.40 | −0.57 ± 0.11 | 0.02 ± 0.34 | 1.7 | | | 4 | 11.0 |
| GAVL | 7.69 | | −1.07 | −1.25 ± 0.16 | −1.03 ± 0.18 | 1.2 | −1.26 ± 0.15 | −0.0 | 44 | 8.9 |
| HELS | 1.41 | | −0.06 | −0.23 ± 0.10 | 1.24 ± 0.92 | 1.6 | | | 5 | 11.5 |
| HONB | 5.04 | | −0.80 | −0.82 ± 0.13 | −0.92 ± 0.21 | −0.6 | | | 4 | 16.7 |
| HONC | 4.94 | 5.14 | −0.78 | −0.81 ± 0.13 | −0.07 ± 0.21 | 3.3 | | | 12 | 15.9 |
| HONN | 2.54 | 2.36 | −0.29 | −0.41 ± 0.11 | −0.38 ± 0.72 | −0.0 | | | 5 | 4.9 |
| JOEN | 3.91 | 3.43 | −0.66 | −0.64 ± 0.12 | −0.56 ± 0.28 | 0.0 | −0.44 ± 0.22 | 0.7 | 9 | 12.7 |
| KAUT | 5.27 | 5.11 | −0.72 | −0.86 ± 0.13 | −2.18 ± 0.67 | −2.0 | | | 5 | 4.9 |
| KEVO | 4.19 | 4.34 | −0.53 | −0.68 ± 0.12 | 0.21 ± 0.46 | 1.8 | | | 6 | 6.0 |
| KIRU | 6.95 | 7.08 | −0.94 | −1.13 ± 0.15 | −0.92 ± 0.17 | 1.1 | −1.13 ± 0.13 | 0.0 | 14 | 20.0 |
| KRAM | 9.83 | 9.75 | −1.33 | −1.60 ± 0.19 | −1.45 ± 0.33 | 0.4 | −1.80 ± 0.25 | −0.7 | 10 | 10.0 |
| KUUB | 7.09 | 7.29 | −1.11 | −1.16 ± 0.15 | −1.28 ± 0.53 | −0.0 | | | 4 | 6.1 |
| LYCK | 9.95 | | −1.29 | −1.62 ± 0.19 | −1.63 ± 0.44 | 0.0 | −1.90 ± 0.33 | −0.7 | 6 | 8.0 |
| MARA | 7.58 | 7.59 | −1.05 | −1.24 ± 0.16 | −1.04 ± 0.12 | 1.4 | −1.29 ± 0.10 | −0.5 | 36 | 38.5 |
| METS | 4.49 | 4.29 | −0.35 | −0.73 ± 0.12 | −0.75 ± 0.05 | −1.0 | | | 223 | 32.4 |
| NMBU | 4.73 | | −0.79 | −0.77 ± 0.13 | −0.56 ± 0.28 | 0.7 | −0.56 ± 0.21 | 0.8 | 10 | 9.8 |
| ONSA | 2.89 | 2.90 | −0.26 | −0.47 ± 0.11 | −0.16 ± 0.09 | 3.0 | −0.30 ± 0.07 | 1.6 | 52 | 21.8 |
| OSTE | 8.56 | 8.64 | −1.10 | −1.40 ± 0.17 | −1.00 ± 0.27 | 1.4 | −1.30 ± 0.20 | 0.6 | 13 | 12.0 |
| RATA | 10.17 | 10.02 | −1.39 | −1.66 ± 0.19 | −1.74 ± 0.44 | −0.2 | −2.01 ± 0.33 | −0.9 | 6 | 8.0 |
| RIGA | 0.85 | 1.24 | −0.08 | −0.14 ± 0.10 | −0.68 ± 0.21 | −2.8 | | | 5 | 18.1 |
| SKEL | 10.12 | 10.31 | −1.41 | −1.65 ± 0.19 | −1.52 ± 0.13 | 0.9 | −1.65 ± 0.10 | 0.4 | 16 | 23.6 |
| SMID | 0.53 | 0.49 | 0.13 | −0.09 ± 0.10 | −2.14 ± 1.58 | −1.3 | | | 3 | 8.0 |
| SMOG | 3.76 | 3.93 | −0.49 | −0.61 ± 0.12 | −0.02 ± 0.32 | 1.7 | −0.35 ± 0.24 | 0.9 | 10 | 10.6 |
| SODA | 7.41 | 7.61 | −1.18 | −1.21 ± 0.16 | −1.58 ± 0.18 | −2.2 | −0.69 ± 0.30 | 1.7 | 13 | 34.9 |
| STVA | 1.56 | 1.39 | −0.11 | −0.25 ± 0.10 | −0.44 ± 0.20 | −1.1 | −0.44 ± 0.15 | −1.7 | 7 | 15.2 |
| SULD | 1.56 | 1.15 | 0.01 | −0.25 ± 0.10 | −0.54 ± 1.16 | −0.3 | | | 4 | 10.3 |
| SUUR | 3.40 | 3.95 | −0.18 | −0.55 ± 0.11 | −0.14 ± 0.38 | 1.0 | | | 4 | 18.1 |
| TORA | 1.33 | 1.21 | −0.05 | −0.22 ± 0.10 | −0.72 ± 0.62 | −0.9 | | | 3 | 12.8 |
| TRDA | 4.71 | | −0.54 | −0.77 ± 0.13 | −1.82 ± 0.22 | −5.0 | | | 10 | 14.8 |
| TRDH | 0.75 | 0.23 | −0.08 | −0.12 ± 0.10 | 1.07 ± 0.55 | 2.1 | | | 6 | 9.7 |
| TROM | 2.87 | 3.13 | −0.12 | −0.47 ± 0.11 | −0.08 ± 0.23 | 1.5 | | | 8 | 15.9 |
| TRYC | 6.91 | 7.15 | −1.02 | −1.13 ± 0.15 | −1.16 ± 0.10 | −0.5 | −1.24 ± 0.08 | −1.5 | 24 | 18.0 |
| VAAA | 9.40 | | −1.28 | −1.53 ± 0.18 | −1.96 ± 0.14 | −3.2 | | | 16 | 24.3 |
| VAAB | 9.26 | 8.41 | −1.26 | −1.51 ± 0.18 | −1.55 ± 0.17 | −0.3 | −1.46 ± 0.13 | 0.5 | 16 | 16.9 |
| VAGA | 2.26 | | −0.17 | −0.37 ± 0.11 | −0.88 ± 0.59 | −0.9 | | | 4 | 7.2 |
| VISB | 3.19 | 3.17 | −0.27 | −0.52 ± 0.11 | −0.36 ± 0.37 | 0.3 | −0.76 ± 0.28 | −1.0 | 6 | 9.1 |
| VLNS | −0.03 | −0.26 | −0.01 | 0.00 ± 0.10 | −0.33 ± 0.35 | −1.1 | | | 4 | 19.4 |
| VVOL | 1.12 | | −0.03 | −0.18 ± 0.10 | −0.35 ± 0.45 | −0.5 | −0.28 ± 0.36 | −0.5 | 11 | 11.0 |

### 2.5 The geophysical GIA model ICE-6G(VM5a)

In addition to using the state of the art Fennoscandian land uplift model NKG2016LU (based on land uplift observations), $\dot{g}$ is also predicted by means of a standard geophysical GIA model, namely ICE6-G(VM5a), which is widely used throughout the world as a reference for land uplift and gravity observations.

The GIA model is based on the viscoelastic normal-mode method, pseudo-spectral approach (Mitrovica *et al.* 1994; Mitrovica & Milne 1998), with an iterative procedure in the spectral domain and spherical harmonic expansion truncated at degree 192 (Steffen & Kaufmann 2005) and applied using the software ICEAGE (Kaufmann 2004). The ice history is according to the ice model ICE-6G_C and earth rheology according to earth model VM5a (Argus *et al.* 2014; Peltier *et al.* 2015). The direct attraction term (from present day, GIA-induced sea level variations) in the Green's function for gravity was omitted, following the recommendations from Olsson *et al.* (2012).

## 3 ESTIMATION OF GRAVITY TRENDS FROM OBSERVATIONS

From the repeated AG observations we estimate $\dot{g}$ at all stations with more than two observations and a time span longer than 2 yr. For comparison, we constructed two different data sets (I and II) based on the observations listed in Table S4. Dataset I includes all observations as they are and Dataset II is refined in such way that observations and stations with large uncertainties and suspected errors are removed (see below). These estimated gravity trends are then

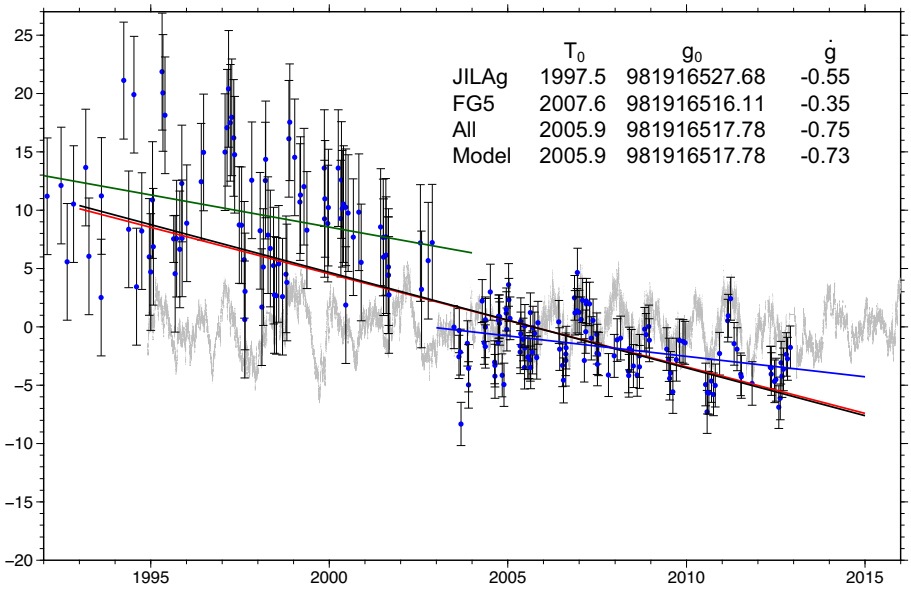


**Figure 4.** Gravity observations and trend lines at the Metsähovi station. The red line shows the gravity trend predicted by $-0.163{\cdot}\dot{h}_{NKG2016LU\_abs}$; the black line is the estimated trend using all observations, the green line (1992–2003) is the trend estimated using only JILAg measurements and the blue line (2003–2012) using only FG5 measurements. For comparison, the grey line shows the detrended SG observations (see also Virtanen *et al.* 2014).

**Table 7.** Statistics for the difference between $\dot{g}_{\mathrm{LU}}$ and the other determinations of $\dot{g}$ in Table 6 ($\mu$Gal yr$^{-1}$).

| $\dot{g}_{\mathrm{LU}}$ minus... | Mean | Std dev | Max | Min | $n_{\mathrm{stns}}$ |
|---|---|---|---|---|---|
| ...$\dot{g}_{\mathrm{GIA}}$ | −0.20 | ±0.11 | 0.02 | −0.38 | 41 |
| ...$\dot{g}_{I}$ | 0.03 | ±0.67 | 2.05 | −1.47 | 41 |
| ...$\dot{g}_{II}$ | 0.03 | ±0.28 | 0.81 | −0.52 | 21 |

compared with NKG2016LU_abs (Section 2.4) and a geophysical GIA model (Section 2.5), shown in Table 6.

*Dataset I* consists of all AG observations as they are listed in Table S4. The gravity rate of change, $\dot{g}$, and a reference gravity value, $g_0$, in the reference epoch, $T_0$ (mean epoch of all observations), are estimated for each station, $i$, by means of weighted least squares adjustment (WLSA) with the observation equations

$$g^{ij}_{\mathrm{obs}} = g^{i}_{0} + (T_0 - T^{j}) \cdot \dot{g}^{i}_{\mathrm{obs}} + \varepsilon^{ij}, \tag{2}$$

where $g^{ij}_{obs}$ is one gravity observation at station $i$ at epoch $T^j$. The observations are weighted with $1/\sigma^2_{\mathrm{tot}}$, where $\sigma_{\mathrm{tot}}$ is the total standard uncertainty as given in Table S4.

In *Dataset II* only FG5 observations are used, that is IMGC, GABL, JILAg, and A10 observations are omitted and only stations with 5 or more observations spanning over at least 5 yr are considered.

The omission of other absolute observations than those made with FG5 is motivated by the fact that FG5 instruments have a lower observational uncertainty than the other types of instruments. Especially, the internal consistency with this group of AGs is high, which is crucial here when repeatability is more important than the absolute level. Using only one type of instrument decreases the risk of introducing (unknown) offsets between instruments. Since the observations with the omitted instruments in general are concentrated to the earliest part of the time-series (except A10), any offsets would greatly impact trend estimates. Except for the JILAg instrument the omitted instruments have contributed with relatively few observations.

In Finland, JILAg#5 was heavily used during the 1990s and early 2000s, especially at the METS station. Fig. 4 shows all observations at METS. Up to 2003 these observations are almost exclusively JILAg type, and after 2003 they are only FG5 type. Three different estimates of $\dot{g}$ at METS are shown in Fig. 4; one using only JILAg observations ($-0.55 \pm 0.18$ $\mu$Gal yr$^{-1}$), one using only FG5 ($-0.35 \pm 0.06$ $\mu$Gal yr$^{-1}$) and one using all available observations ($-0.75 \pm 0.05$ $\mu$Gal yr$^{-1}$). Using all observations, the estimated $\dot{g}$ agrees very well with the rate predicted by the NKG2016LU_abs model. The FG5 trend differs significantly from the trend based on all observations and one reason could be a possible offset between the JILAg#5 and FG5 instruments. Introducing this offset as an unknown in the observation equation (eq. 2) gives an estimate of the offset between JILAg#5 and FG5 of 7.74±0.78 $\mu$Gal and, at METS, $\dot{g} = -0.41 \pm 0.06$ $\mu$Gal yr$^{-1}$ and $\dot{g}/\dot{h} = -0.092 \pm 0.013$ $\mu$Gal mm$^{-1}$. The results from international comparisons (Table 5) indicate that the bias for JILAg#5 might have changed over the years, but these numbers are not significant and the bias for JILAg#5 is therefore not taken into account in this work (applies to Dataset I).

Since the FG5 trend (as well as the JILAg trend and the trend corrected for an offset) differs significantly from the land uplift model and because of the problem with the suspected offset between the JILAg and FG5 observations, the METS station is excluded from Dataset II. HONC, TRDA and TROM (Ophaug *et al.* 2016) and VAAA and KEVO have been pointed out to have gravity trends induced by multiple overlapping processes thus hiding the GIA signal. They are therefore also omitted from Dataset II.

In Dataset II, the shift identified in the FG5#233 time-series (see Section 2.3) is corrected according to method 3c in Olsson *et al.* (2016), that is, with the DoE reported from the international comparisons (Table 5).

The adjustment of the data in Dataset II is conducted the same way as for Dataset I (eq. 2). Two observations (TRYB 2008.254, MARA 2013.485) are identified as outliers (deviate more than $3\sigma_{\mathrm{tot}}$ from the estimated trendline) and are therefore removed.

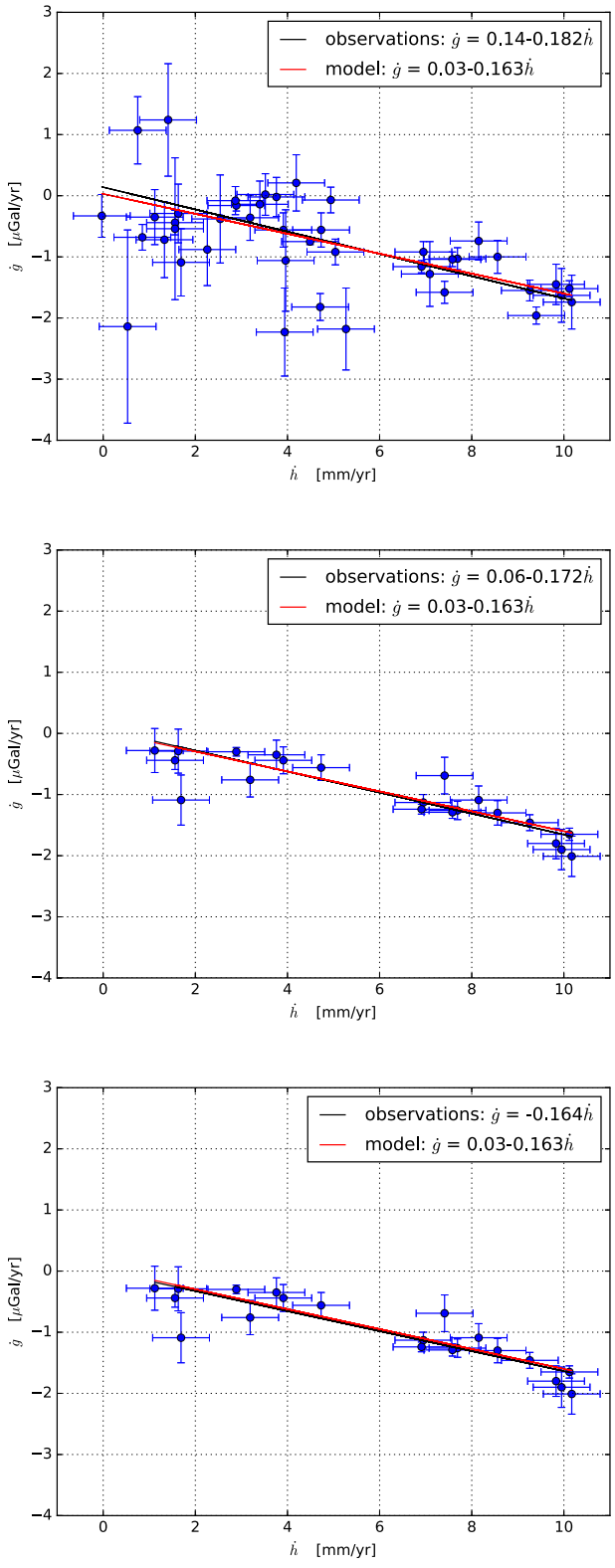


**Figure 5.** Plot of $\dot{g}$ versus $\dot{h}$ (NKG2016LU_abs). Each blue dot corresponds to one AG station. The error bars show the standard uncertainty ($1\sigma$) of $\dot{g}$ and $\dot{h}$. Black line shows the empirical relation from observations (WODR) and red line the geophysical relation from GIA model. Top panel shows Dataset I, middle Dataset II and lower panel shows Dataset II where the trend line is forced through the origin.

At stations with observations on more than one pillar (METS, MARA, ONSA, TRYC) the observations on the individual pillars have been merged to one, in the adjustment, by assuming the same $\dot{g}$-value on all pillars and estimating an additional parameter for gravity difference between the pillars.

The difference between Dataset I and II (Table 6) can be explained in different ways for different countries. In Finland and the Baltic countries the difference is primarily because of the exclusion of the JILAg data, in Denmark the exclusion of A10 data and in Sweden because of the correction for the identified shift in the FG5#233 time-series.

$\dot{g}_{\mathrm{GIA}}$ in Table 6 represents the global GIA model ICE-6G(VM5a), described in Section 2.5. It is included here to show how such a model performs compared to observational data. Table 7 shows the difference between gravity change predicted using the empirical model, NKG2016LU, and the other predictions/estimates of $\dot{g}$. For $\dot{g}_{\mathrm{GIA}}$ the standard deviation is smaller compared to the observed rates but on average the AG-observations fit better with the empirical model, that is other types of geodetic observations in the area. $\dot{g}_{\mathrm{GIA}}$ is not specifically tuned to Fennoscandia and modern GIA observations there and systematically underestimates the gravity change (is less negative) compared to both AG-observations and NKG2016LU. Below NKG2016LU will be used as the reference model.

## 4 THE RELATION BETWEEN $\dot{g}$ AND $\dot{h}$

For evaluation of the geophysical relation between $\dot{g}$ and $\dot{h}$ (eq. 1), we apply both WLSA and WODR methods to estimate $\dot{g}_0$ and $C$ in

$$\dot{g}^i = \dot{g}_0 + C \cdot \dot{h}^i + \varepsilon^i \tag{3}$$

from observations. The first method allows errors in the observations ($\dot{g}$) to be taken into account, while the latter considers also errors in the regressor ($\dot{h}$). In eq. (3), $\dot{g}^i$ is $\dot{g}$ from Table 6 for station $i$ and $\dot{h}^i$ is the corresponding land uplift value from NKG2016LU_abs.

The standardized residuals, given in Table 6, are

$$\bar{\varepsilon}^i = \frac{\varepsilon^i}{\sigma_{\dot{g}}^i} \tag{4}$$

from the WLSA solution. They indicate if the residual between the estimated $\dot{g}$-value for the station in question ($\dot{g}^i$) and the trend line ($\dot{g} = \dot{g}_0 + C \cdot \dot{h}$) is smaller ($<1$) or larger ($>1$) than the estimated standard uncertainty for that $\dot{g}$-value. For example $\bar{\varepsilon}^i > 3$ indicates that the estimated $\dot{g}^i$-value deviates more than $3\sigma$ from the trend line.

Using WODR, the minimization problem is defined as (Boggs *et al.* 1992)

$$\min \sum_i^n \left( w_{\epsilon_i} \epsilon_i^2 + w_{\delta_i} \delta_i^2 \right), \tag{5}$$

where $w_{\epsilon_i}$ and $\varepsilon_i$ are the weight and the residual of $\dot{g}_i$, and $w_{\delta_i}$ and $\delta_i$ are the weight and the residual of $\dot{h}_i$. For both $\dot{g}$ and $\dot{h}$ the weights were set equal the inverse of the squared standard error. We used the ODR-package (Boggs *et al.* 1992) of the Python library SciPy to solve the minimization problem defined in eq. (5). Using WODR we circumvent a systematic bias that is introduced if we use WLSA for line fitting when there is uncertainty in the predictor (Pitkänen *et al.* 2016). Because WLSA aims to minimize the vertical distance between data points and the fitting line, a larger horizontal spread of the predictor will cause the fitting line to accommodate

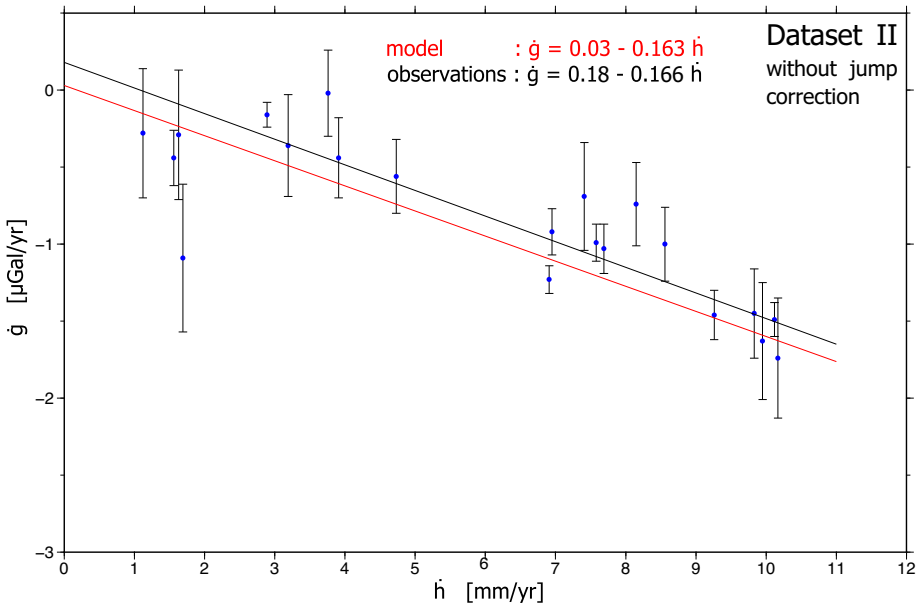


**Figure 6.** Systematic errors in the gravity trends will cause offsets of the $\dot{g}/\dot{h}$ trend line ($\dot{g}_0 \neq 0$). The figure shows the trend line for Dataset II not corrected for the jump in the FG5#233 time-series.

**Table 8.** Summary of theoretical and estimated relations between $\dot{g}$ and $\dot{h}$. Given uncertainties correspond to the standard uncertainty (one sigma). The relation was estimated by WLSA and WODR.

| Relation | $\dot{g}_0$ | $C$ | Estimator |
|---|---|---|---|
| Geophysical | 0.03 | $-0.163 \pm 0.016$ | GIA model |
| Dataset I | $0.05 \pm 0.12$ | $-0.167 \pm 0.020$ | WLSA |
| Dataset I | $0.14 \pm 0.14$ | $-0.181 \pm 0.022$ | WODR |
| Dataset II | $0.10 \pm 0.09$ | $-0.177 \pm 0.013$ | WLSA |
| Dataset II | $0.06 \pm 0.10$ | $-0.172 \pm 0.015$ | WODR |
| Dataset II, forced through origin | $0.00 \pm 0.00$ | $-0.163 \pm 0.005$ | WLSA |
| Dataset II, forced through origin | $0.00 \pm 0.00$ | $-0.164 \pm 0.006$ | WODR |
| Dataset II, $\dot{h}$ from GNSS | $0.04 \pm 0.12$ | $-0.168 \pm 0.017$ | WODR |

by sloping (or attenuating) towards zero. This mechanism is known as the attenuation or regression dilution bias (e.g. Hutcheon *et al.* 2010; Van Camp *et al.* 2016a). By contrast, WODR is an example of a bivariate regression technique which takes uncertainties of both outcome and predictor into account, and minimizes the shortest distance between data points and the vertical line. As such, the mechanism causing the regression dilution bias never occurs.

In Fig. 5, all the estimated gravity rates from Table 6 are plotted against their corresponding land uplift value (NKG2016LU_abs), for both data sets. Also the estimated linear relations (WODR) as well as the geophysical relation (eq. 1) are plotted. The bottom panel of Fig. 5 shows the trend for Dataset II forced through the origin, that is $\dot{g}_0 = 0$. It is clear from eq. (1) that the GIA-model predicts a small deviation of $\dot{g}_0$ from 0. Still, most of earlier studies of this relation (Table 2) have assumed $\dot{g}_0 = 0$ and therefore we include that here for comparison.

Collilieux *et al.* (2014) and Mazzotti *et al.* (2011), for example, use $\dot{g}_0$ for evaluation of systematic errors in $\dot{h}$ based on the assumption that $\dot{g}_0 \neq 0$ would indicate systematic errors in the scale and centre of mass of the GNSS reference frame. It should be noticed that also systematic errors in the gravity rates would result in offsets of the trend line. The identified shift in the time-series of FG5#233 (see Section 3) caused systematically lower estimates of the gravity rates in Sweden. Dataset II is corrected for that shift but Fig. 6 shows the trend line WLSA for Dataset II without this correction.

Although NKG2016LU is our preferred solution for $\dot{h}$, we have also fit eq. (3) to Dataset II combined with $\dot{h}$ derived from the BIFROST GNSS observations. This implies that the weights for $\dot{h}$ in the WODR algorithm vary between the stations, in contrast to $\dot{h}$ from NKG2016LU which all have the same weights (0.6164 mm yr$^{-1}$). Note that for four of the stations in Dataset II $\dot{h}$ from GNSS is not available as they are not a part of the BIFROST network and therefore not included in this solution (see Table 6).

Table 8 summarizes the results for different combinations of data sets, sub-sets of stations and estimators. The results indicate that the differences between estimates calculated with WLSA and WODR are small, that is, within one sigma for both Dataset I and II.

The empirical results are well within the 95 per cent confidence interval of the geophysical relation and all the empirical relations are smaller (more negative) than the geophysical. The estimates of $C$ based on Dataset II range from $-0.163$ to $-0.177$ $\mu$Gal mm$^{-1}$ and agree within the geohysical/modelled value's standard error. The agreement between the solutions indicates that the estimates based on Dataset II are quite robust considering weighting strategy and regression method.

## 5 DISCUSSION

We have used the complete data sets to estimate homogenous relations between $\dot{g}$ and $\dot{h}$ for the region. Of course, ratios between

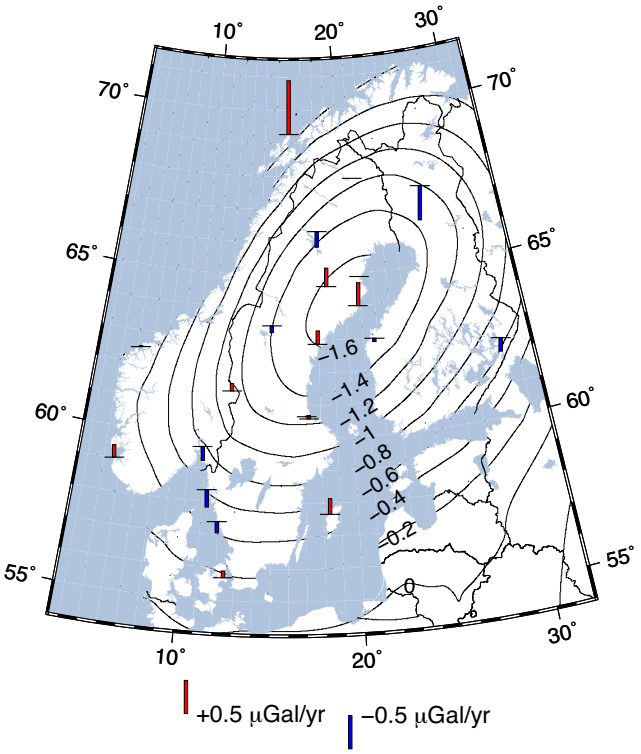


**Figure 7.** NKG2016LU_gdot (isolines) ($\mu$ Gal yr$^{-1}$). Bars show the difference between modelled and observed $\dot{g}$-values (NKG2016LU_gdot$-\dot{g}_{II}$).

$\dot{g}$ and $\dot{h}$ can also be estimated station-wise, but the uncertainties in the observations are (still) too large for this to be meaningful, especially when $\dot{h}$ and $\dot{g} \rightarrow 0$.

Also the uncertainties of estimated $\dot{g}$ (Table 6) are, in general, large compared to the uncertainties of the land uplift model. This is due to the fact that there are still quite few gravity observations at most stations ($\leq$5 for 40 per cent of the stations) and that there are unmodelled local effects, possibly due to local hydrology or sea level variations (for stations very close to the sea), that may introduce both random and systematic errors in the gravity time-series (Van Camp *et al.* 2016b). Van Camp *et al.* (2005) show that with annual or semiannual AG observations we can expect a standard error of ~0.1 $\mu$Gal yr after 15–25 yr. This is in agreement with the uncertainty for $\dot{g}_{\mathrm{LU}}$ in Table 6 but, due to few observations and shorter time spans, only a few of the observational rates are close to this.

Not only is the uncertainty of the land uplift model still smaller than the uncertainty of the observational AG rates, it is also carefully interpolated (and extrapolated) between the points of observations which allows us to predict $\dot{g}$ at any location (important e.g. for reduction of gravity observations in general to a certain epoch). Still, we need to choose a relation between $\dot{h}$ and $\dot{g}$ in order to convert the land uplift model to gravity. The observational and geophysical relations agree within the uncertainty limits, giving us increased confidence in the latter. This suggests it is safe to use the geophysical (modelled) relation between $\dot{g}$ and $\dot{h}$ in combination with NKG2016LU_abs to convert vertical rates to gravity change. We call this model NKG2016LU_gdot and it is consequently defined as

$$\mathrm{NKG2016LU\_gdot} = -0.163 \cdot \mathrm{NKG2016LU\_abs}\ (\mu\mathrm{Gal\,yr}^{-1}) \quad (6)$$

Worth noticing about the NKG2016LU_gdot is that it is valid in the whole Fennoscandian land uplift area but not on, or very close to the sea. There the relation between $\dot{g}$ and $\dot{h}$ is different because of the direct attraction from GIA-induced sea level variations, and depends on the physical location of the station relative to the sea. Olsson *et al.* (2015) show that for stations located closer to the sea than 10 times the height of the station this effect should be considered and requires a local and rigorous treatment (see e.g. Lysaker *et al.* 2008; Breili 2009; Olsson *et al.* 2009; Breili *et al.* 2010; Olsson *et al.* 2012).

In Fig. 7, NKG2016LU_gdot is plotted together with the difference between this model and the observational $\dot{g}$-values from Dataset II, $\dot{g}_{II}$ (Table 6). The deviations of the observational results from the model are well within the 95 per cent uncertainty level of the estimated $\dot{g}$ (cf. Fig. 5). Close to the land uplift maximum there are three stations (SKEL, LYCK and RATA) where the observed value is larger (more negative) than the model. This is partly explained by Olsson *et al.* (2016) as a consequence of the introduced correction for the jump in combination with few observations after 2013. The large positive anomaly of $\dot{g}$ at ANDO indicates that the observed gravity change signal is dominated by other processes than GIA, for example, tectonics or varying hydrology (Ophaug *et al.* 2016).

Fig. 8 shows the difference between NKG2016LU_gdot and NKG2016LU_abs converted to $\dot{g}$ using the observational relation, $\dot{g} = 0.06 - 0.172\dot{h}$ (Dataset II, WODR). The difference in Fennoscandia is smaller than $\pm$0.05 $\mu$Gal yr$^{-1}$ which means that for 20 yr of epoch reduction, using one or the other model, the difference will be smaller than 1 $\mu$Gal.

Finally, we make a comparison of the results in Table 6 with the results from land uplift gravity lines (Fig. 1). Mäkinen *et al.* (2005) presented the $\dot{g}$ difference between VAGA and KRAM along the western part of the 63° line and between VAAB and JOEN along eastern part. On the western part VAGA has been excluded from Dataset II because of too few observations so here the results from Dataset I are used. Table 9 summarizes this comparison and the conclusion is that within the uncertainties all results agree. Since AG observations give different trends at VAAA and VAAB (Table 6) this also confirms that the AG trend at VAAA probably consists of more than the GIA signal.

## 6 CONCLUSIONS

For the first time, all repeated AG observations (1976–2015) in the Fennoscandian land uplift area were compiled and presented. This means 688 observations at 59 stations across the region. Ten different organizations have contributed with data spanning for more than three decades. The primary application of the observations is to study the GIA-induced gravity rate of change, $\dot{g}$. This study also clearly demonstrates the possibility to determine the $\dot{g}/\dot{h}$ ratio with sufficient precision to validate corresponding results from, for example, GIA models and to be used for converting absolute land uplift values, $\dot{h}$, to surface gravity change, $\dot{g}$.

For all stations with more than two observations and a time span longer than 2 yr, $\dot{g}$ was estimated and compared to predicted values. Two data sets were derived; Dataset I corresponds to all original data and Dataset II is modified with the intention to reduce effects from known or possible systematic or gross errors and includes only FG5 observations. $\dot{g}$ was also determined at all AG stations using (i) the semi-empirical land uplift model NKG2016LU and (ii)

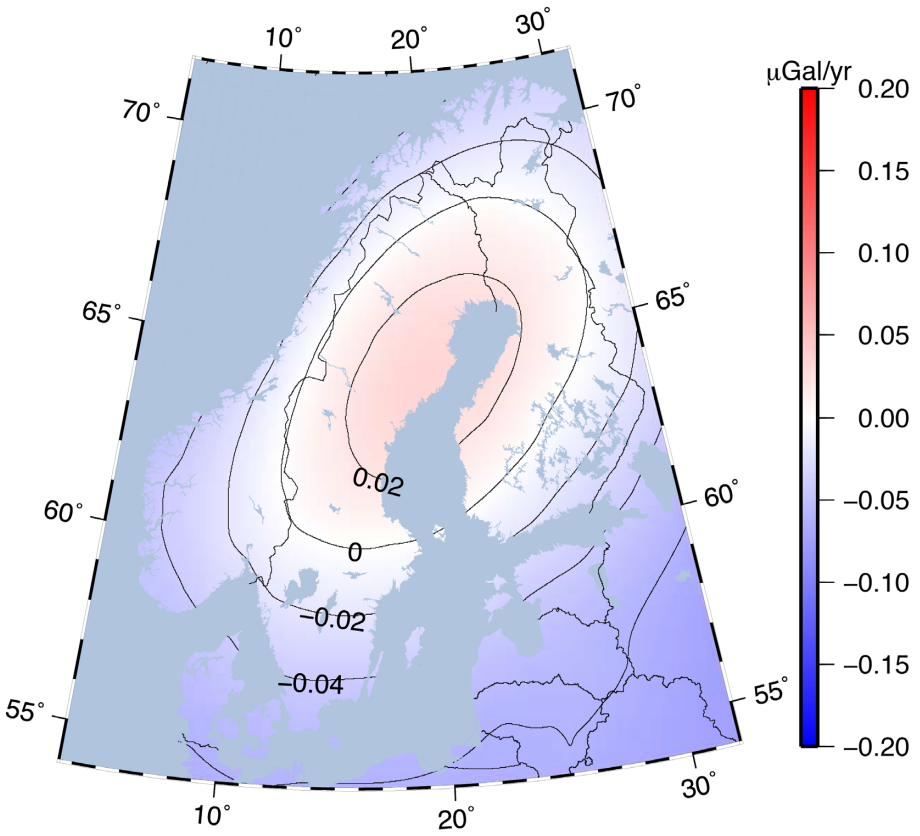


**Figure 8.** Difference between $\dot{g}$-models: NKG2016LU_gdot$-\dot{g}_{obs}$, where $\dot{g}_{obs}$ is NKG2016LU_abs converted to $\dot{g}$ using the relation-based geodetic AG observations, $\dot{g} = 0.06 - 0.172\dot{h}$ (Dataset II, WODR).

**Table 9.** Comparison of relative ($\dot{g}_{RG}$), absolute ($\dot{g}_{AG}$) and modelled ($\dot{g}_{LU}$) results along the 63° land uplift gravity line. All numbers in μGal yr$^{-1}$.

| | VAGA-KRAM | VAAB-JOEN |
|---|---|---|
| $\Delta\dot{g}_{RG}$ | $1.07 \pm 0.24$ | $0.91 \pm 0.09$ |
| $\Delta\dot{g}_{AG}$ | $0.92 \pm 0.64$ | $1.02 \pm 0.26$ |
| $\Delta\dot{g}_{LU}$ | $1.23 \pm 0.22$ | $0.89 \pm 0.22$ |

a geophysical GIA model based on the ice model ICE-6G_C and VM5a earth rheology.

NKG2016LU was chosen as reference model and the mean differences between this model and the empirical values are not significantly deviating from zero ($0.03 \pm 0.67$ and $0.03 \pm 0.28$ μGal yr$^{-1}$ for Dataset I and Dataset II, respectively). The standard deviation for the difference between the reference model and the GIA model is smaller, 0.11 μGal yr$^{-1}$, but the GIA model systematically underestimates the gravity change.

A linear relation, $\dot{g} = \dot{g}_0 + C \cdot \dot{h}$, valid for the entire region, between $\dot{g}$ and $\dot{h}$ (NKG2016LU) was determined by means of WLSA and WODR for each data set. The difference between estimates calculated with WLSA and WODR is small, that is within 1 $\sigma$. Dataset II results in smaller standard deviations and estimates of $C$ from Dataset II range from $-0.163$ to $-0.177$ μGal mm$^{-1}$. Estimates of the constant part are not significantly different from zero. All empirical results are smaller than, and well within the 95 per cent confidence interval of, the geophysical relation $\dot{g} = 0.03 - 0.163\dot{h}$. This implies that using the geophysical relation is a reasonable choice. Just using the simple ratio $\dot{g}/\dot{h} = -0.163$ (μGal mm$^{-1}$) will differ from using the full relation only by 0.03 μGal yr$^{-1}$, that is <1 μGal over 30 yr, and may be a reasonable choice for practical applications. This also exactly coincides with estimates of $C$ (Dataset II) when $\dot{g}_0$ is assumed to be zero.

The uncertainty of $\dot{g}$ estimated from observations at the gravity stations is relatively high and inhomogeneous (∼0.1−0.6 μGal yr$^{-1}$) when compared to the lower and more homogenous uncertainty obtained by predicting $\dot{g}$ from land uplift observations by means of the land uplift model NKG2016LU_abs (0.1–0.2 μGal yr$^{-1}$). In addition, the gravity observations are geographically limited to a few discrete points while the land uplift model comes as an interpolated surface (grid) covering the entire region. At present, we therefore recommend using the latter, which we call NKG2016LU_gdot (= −0.163·NKG2016LU_abs), as the most reliable and suitable method to predict the GIA-induced gravity change in Fennoscandia. A gridded version of NKG2016LU_gdot can be downloaded at https://www.lantmateriet.se/en/maps-and-geographic-information/GPS-och-geodetisk-matning/Referenssystem/Landhojning/.

Continuation of the AG observations at the stations already established is important in order to decrease the uncertainty and enable more accurate determinations of the relation to the land uplift. This will also improve the possibilities to descriminate the GIA signal from other environmental signals.

## ACKNOWLEDGEMENTS

We would like to express our thanks to all organizations and all people that contributed with absolute gravity observations over the years.

Besides the organizations represented by the authors we would especially like to thank BKG and NOAA which took part in the beginning of the project and contributed with valuable early observations.

Thank you, for your important contributions, Linda Alm, Ove Christian Dahl Omang, Fredrik Dahlström, Bjørn Engen, Andreas Engfeldt, Reinhard Falk, René Forsberg, Christian Gerlach, Olga Gitlein, Walter Hoppe, Fred Klopping, Géza Lohasz, Dagny Iren Lysaker, Jürgen Müller, Jaakko Mäkinen, Jyri Näränen, Are Jo Næss, Jon Glenn Omholt Gjevestad, Bjørn Ragnvald Pettersen, Gunnar Regevik, Andreas Reinhold, Erik Roland, Hannu Ruotsalainen, Knut Røthing, Glenn Sasagawa, Hans-Georg Scherneck, Marcin Sekowski, Gabriel Strykowski, Runar Svensson, Herbert Wilmes, Walter Zürn, Jonas Ågren, Ola Øvstedal and all others that in one way or the other contributed to this work.

We are also grateful to Michel van Camp and Hartmut Wziontek, whose reviews have greatly helped in improving our manuscript.

## REFERENCES

Ågren, J. & Svensson, R., 2007. Postglacial land uplift model and system definition for the new Swedish height system RH 2000. , LMV-Rapport 2007:4, Lantmäteriet.

Argus, D.F., Peltier, W.R., Drummond, R. & Moore, A.W., 2014. The Antarctica component of postglacial rebound model ICE-6G_C (VM5a) based on GPS positioning, exposure age dating of ice thicknesses, and relative sea level histories, *Geophys. J. Int.,* **198,** 537–563.

Arnautov, G.P., Boulanger, Yu.D., Kalish, E.N., Koronkevitch, V.P., Stus, Yu.F. & Tarasyuk, V.G., 1983. Gabl, an absolute free-fall laser gravimeter, *Metrologia,* **19**(2), 49.

Bilker-Koivula, M., Mäkinen, J., Timmen, L., Gitlein, O., Klopping, F. & Falk, R., 2008, Repeated absolute gravity measurements in Finland, in *International Symposium Terrestrial Gravimetry: Static and Mobile Measurements, State Research Center of Russia Elektropribor,* pp. 147–151, ed.Peshekhonov, International Association of Geodesy, St. Petersburg, Russia.

Boggs, P.T., Byrd, R.H., Rogers, J.E. & Schnabel, R.B., 1992. User's reference guide for ODRPACK version 2.01 software for weighted orthogonal distance regression, Tech. Rep., Department of Commerse, Technology Administration, National Instiute of Standards and Technology. Available at:https://docs.scipy.org/doc/external/odrpack_guide.pdf, Accessed 2019-02-13.

Boulanger, Y.D., Amautov, G.P. & Scheglov, S.N., 1983. Results of comparison of absolute gravimeters, Sevres, 1981, *Bull. Inf. Bur. Grav. Int.,* **52,** 99–124.

Boulanger, Y. *et al.*, 1986. Results of the second international comparison of absolute gravimeters in Sevres, 1985, *Bull. Inf. Bur. Grav. Int.,* **59,** 89–103.

Boulanger, Y. *et al.*, 1991. Results of the third international comparison of absolute gravimeters in Sevres, 1989., *Bull. Inf. Bur. Grav. Int.,* **68,** 24–44.

Breili, K., 2009. *Investigations of surface loads of the Earth - geometrical deformations and gravity changes,* PhD thesis, Norwegian University of Life Sciences, Ås.

Breili, K., Gjevestad, J.G., Lysaker, D.I., Dahl Omang, O.C. & Pettersen, B.R., 2010. Absolute gravity values in Norway, *Norsk Geografisk Tidsskrift - Norwegian J. Geogr.,* **64,** 79–84.

Collilieux, X. *et al.*, 2014. External evaluation of the terrestrial reference frame: report of the task force of the IAG sub-commission 1.2, in *Earth on the Edge: Science for a Sustainable Planet: Proceedings of the IAG General Assembly, Melbourne, Australia, June 28-July 2, 2011,* Vol. **139,** pp. 197–202, eds Rizos, C. & Willis, P., *International Association of Geodesy Symposia Series,* Springer-Verlag.

de Linage, C., Hinderer, J. & Boy, J.-P., 2009. Variability of the gravity-to-height ratio due to surface loads, *Pure appl. Geophys.,* **166,** 1217–1245.

Ekman, M., 1991. A concise history of the postglacial land uplift research (from its beginning to 1959), *Terra Nova,* **3,** 358–365.

Ekman, M., 1996. A consistent map of the postglacial uplift of Fennoscandia, *Terra Nova,* **8,** 158–165.

Ekman, M. & Mäkinen, J., 1996. Resent postglacial rebound, gravity change and mantle flow in Fennoscandia, *Geophys. J. Int.,* **126,** 229–234.

Engfeldt, A. *et al.*, 2006. Observing absolute gravity acceleration in the Fennoscandian land uplift area, in *1st International Symposium of the International Gravity Field Service (IGFS' 06),* August 28–September 1, Istanbul, Turkey .

Fang, M. & Hager, B.H., 2001. Vertical deformation and absolute gravity, *Geophys. J. Int.,* **146**(2), 539–548.

Francis, O. & van Dam, T., 2006. Analysis of results of the international comparison of absolute gravimeters in Walferdange (Luxembourg) of November 2003, *Cahiers du Centre Européen de Géodynamique et de Séismologie,* **26,** 1–23.

Francis, O. *et al.*, 2010. Results of the European comparison of absolute gravimeters in Walferdange (Luxembourg) of November 2007, in *Gravity, Geoid and Earth Observation: IAG Commision 2: Gravity Field, Chania, Crete, Greece, 23-27 June 2008,* Vol. **135,** pp. 31–35, ed. Mertikas, S.P., *International Association of Geodesy Symposia Series,* Springer-Verlag.

Francis, O. *et al.*, 2013. The European comparison of absolute gravimeters 2011 (ECAG-2011) in Walferdange, Luxembourg: results and recommendations, *Metrologia,* **50,** 257–268.

Francis, O. *et al.*, 2015. CCM.G-K2 key comparison, *Metrologia,* **52**(1A), 07009. doi:10.1088/0026-1394/52/1a/07009

Germak, A., Capelli, A., DAgostino, G., Desogus, S., Origlia, C. & Quagliotti, D., 2006. A transportable absolute gravity meter adopting the symmetric rise and falling method, in *Proceedings of the XVIII IMEKO World Congress, Metrology for a Sustainable Development,* September 17–22, 2006, Rio de Janeiro, Brazil.

Gitlein, O., 2009. *Absolutgravimetrische Bestimmung der Fennoskandischen Landhebung mit dem FG5-220,* PhD thesis, Leibniz Universität Hannover.

Haller, L.Å. & Ekman, M., 1988. *The Fundamental Gravity Network of Sweden,* Tekniska skrifter - Professional Paper, 1988:16, Lantmäteriet, National Land Survey.

Hutcheon, J.A., Chiolero, A. & Hanley, J.A., 2010. Random measurement error and regression dilution bias, *BMJ,* **340,** c2289, doi:10.1136/bmj.c2289.

IAG, 1984. Resolutions of the XVIII General Assembly of the International Association of Geodesy, Hamburg, Germany, August 15-27, 1983, *J. Geod.,* **58**(3), 309–323.

James, T. & Ivins, E., 1998. Predictions of Antarctic crustal motions driven by present-day ice sheet evolution and by isostatic memory of the Last Glacial Maximum, *J. geophys. Res.,* **103**(B3), 4993–5017.

Jiang, Z. *et al.*, 2011. Final report on the seventh international comparison of absolute gravimeters (ICAG 2005), *Metrologia,* **48,** 246–260.

Jiang, Z. *et al.*, 2012. The 8th international comparison of absolute gravimeters 2009: the first key comparison (CCM.G-K1) in the field of absolute gravimetry, *Metrologia,* **49,** 666–684.

Johansson, J.M., 2002. Continous GPS measurements of postglacial adjustment in Fennoscandia 1. Geodetic results, *J. geophys. Res.,* **107**(B8), ETG 3–1-ETG 3-27.

Kaufmann, G., 2004. *Program Package ICEAGE, version 2004,* Institut für Geophysik der Universität Göttingen, p. 40.

Kierulf, H.P., Steffen, H., Simpson, M.J.R., Lidberg, M., Wu, P. & Wang, H., 2014. A GPS velocity field for Fennoscandia and a consistent comparison to glacial isostatic adjustment models, *J. geophys. Res.,* **119,** 6613–6629.

Kiviniemi, A., 1974. High precision measurements for studying the secular variation in gravity in Finland, *Publ. Finn. Geodet. Inst.,* **78**.

Lambeck, K., Smither, C. & Johnston, P., 1998. Sea-level change, glacial rebound and mantle viscosity for northern Europe, *Geophys. J. Int.,* **134,** 102–144.

Lambeck, K., Purcell, A., Zhao, J. & Svensson, N.-O., 2010. The Scandinavian ice sheet: from MIS 4 to the end of the last glacial maximum, *Boreas,* **39,** 410–435.

Lambert, A., Courtier, N., Sasagawa, G., Klopping, F., Winester, D., James, T. & Liard, J., 2001. New constraints on Laurentide postglacial rebound from absolute gravity measurements, *Geophys. Res. Lett.,* **28**(10), 2109–2112.

Lambert, A., Courtier, N. & James, T.S., 2006. Long-term monitoring by absolute gravimetry: tides to postglacial rebound, *J. Geodyn.,* **41,** 307–317.

Lambert, A., Henton, J., Mazzotti, S., Huang, J., James, T.S., Courtier, N. & van der Kamp, G., 2013a. Postglacial rebound and total water storage variations in the Nelson River drainage basin: a gravity-GPS study, *Open-File 7317,* Natural Resources Canada, Geological Survey of Canada, p. 21

Lambert, A., Huang, J., Kamp, G., Henton, J., Mazzotti, S., James, T.S., Courtier, N. & Barr, A.G., 2013b. Measuring water accumulation rates using GRACE data in areas experiencing glacial isostatic adjustment: The Nelson River basin, *Geophys. Res. Lett.,* **40**(23), 6118–6122.

Larson, K. & van Dam, T., 2000. Measuring postglacial rebound with GPS and absolute gravity, *Geophys. Res. Lett.,* **27**(23), 3925–3928.

Liard, J., Henton, J., Gagnon, C., Lambert, A. & Courtier, N., 2003. Comparison of absolute gravimeters using simultaneous observations, Cahiers du Centre Européen de Géodynamique et de Séismologie, 22, Luxembourg.

Lidberg, M., Johansson, J.M., Scherneck, H.-G. & Davis, J.L., 2007. An improved and extended GPS-derived 3D velocity field of the glacial isostatic adjustment (GIA) in Fennoscandia, *J. Geod.,* **81**(3), 213–230.

Lidberg, M., Johansson, J.M., Scherneck, H.-G. & Milne, G.A., 2010. Recent results based on continuous GPS observations of the GIA process in Fennoscandia from BIFROST, *J. Geodyn.,* **50,** 8–18.

Lysaker, D.I., Breili, K. & Pettersen, B.R., 2008. The gravitational effect of ocean tide loading at high latitude coastal stations in Norway, *J. Geod.,* **82,** 569–583.

Jekeli, C., Bastos, L. & Fernandes, J. Mäkinen, J., Engfeldt, A., Harsson, B.G., Ruotsalainen, H., Strykowski, G., Oja, T. & Wolf, D., 2005. The Fennoscandian land uplift gravity lines 1966–2004, in *IAG International Symposium "Gravity, Geoid, and Space Missions" (GGSM'04), Porto, Portugal, August 30 to September 3, 2004,* IAG Symposia 129, pp. 328–332, Springer, Berlin Heidelberg.

Mäkinen, J., Bilker-Koivula, M., Klopping, F., Falk, R., Timmen, L. & Gitlein, O., 2006, Time series of absolute gravity in Finland, in*1st Internationl Symposium of the International Gravity Field Service (IGFS'06),* August 28–September 1, Istanbul, Turkey.

Mäkinen, J. *et al.*, 2010, Repeated absolute and relative gravity measurements in Fennoscandian postglacial rebound area: comparison of gravity change with observed vertical motion and with GIA models, in*Proc. EGU General Assembly,* Vienna, Austria, 3 pp. .

Marson, I. *et al.*, 1995. Fourth intemational comparison of absolute gravimeters., *Metrologia,* **32,** 137–144.

Mazzotti, S., Lambert, A., Henton, J., James, T.S. & Courtier, N., 2011. Absolute gravity calibration of GPS velocities and glacial isostatic adjustment in mid-continent North America, *Geophys. Res. Lett.,* **38,** L24311, doi:10.1029/2011GL049846.

Memin, A., Hinderer, J. & Rogister, Y., 2012. Separation of the geodetic consequences of past and present ice-mass change: influence of topography with application to Svalbard (Norway), *Pure appl. Geophys.,* **169,** 1357–1372.

Micro-g, LaCoste, 2008. *A10 portable gravimeter user's manual,* Micro-g LaCoste, Lafayette, Colorado, USA.

Micro-g, LaCoste, 2012. *g9 User's Manual,* Micro-g LaCoste, Lafayette, Colorado, USA.

Milne, G.A., Mitrovica, J.X., Scherneck, H.-G., Davis, J.L., Johansson, J.M., Koivula, H. & Vermeer, M., 2004. Continuous GPS measurements of postglacial adjustment in Fennoscandia: 2. Modeling results, *J. geophys. Res.,* **109**(B02412), doi:10.1029/2003JB002619.

Mitrovica, J.X. & Milne, G.A., 1998. Glaciation-induced perturbations in the Earth's rotation: a new appraisal, *J. geophys. Res.,* **103**(B4), 985–1005.

Mitrovica,J.X, Davis, J.L. & Shapiro, I.I., 1994. A spectral formalism for computing three-dimensional deformations due to surface loads 1. Theory, *J. geophys. Res.,* **99**(B4), 7057–7073.

Müller, J., Naeimi, M., Gitlein, O., Timmen, L. & Denker, H., 2012. A land uplift model in Fennoscandia combining GRACE and absolute gravimetry data, *Phys. Chem. Earth,* **53-54,** 54–60.

Niebauer, T.M., Hoskins, J.K. & Faller, J.E., 1986. Absolute gravity: a reconnaissance tool for studying vertical crustal motions, *J. geophys. Res.,* **91**(B9), 9145–9149.

Niebauer,T.M, Sasagawa, G.S., Faller, J.E., Hilt, R. & Klopping, F., 1995. A new generation of absolute gravimeters, *Metrologia,* **32,** 159–180.

Nordman, M., Poutanen, M., Kairus, A. & Virtanen, J., 2014. Using the Nordic Geodetic Observing System for land uplift studies, *Solid Earth,* **5,** 673–681.

Olsson, P.-A., Scherneck, H.-G. & Ågren, J., 2009. Effects on gravity from non-tidal sea level variations in the Baltic Sea, *J. Geodyn.,* **48,** 151–156.

Olsson, P.-A., Ågren, J. & Scherneck, H.-G., 2012. Modelling of the GIA-induced surface gravity change over Fennoscandia, *J. Geodyn.,* **61,** 12–22.

Olsson, P.-A., Milne, G., Scherneck, H.-G. & Ågren, J., 2015. The relation between gravity rate of change and vertical displacement in previously glaciated areas, *J. Geodyn.,* **83,** 76–84.

Olsson, P.-A., Engfeldt, A. & Ågren, J., 2016. Investigations of a suspected jump in the Swedish repeated absolute gravity time series, in *International Symposium on Earth and Environmental Sciences for Future Generations. International Association of Geodesy Symposia,* Vol. **147** , Springer.

Ophaug, V., Breili, K., Gerlach, C., Omholt Gjevestad, J.G., Lysaker, D.I., Pettersen, B.R. & Omang, O.C.D., 2016. Absolute gravity observations in Norway (1993-2014) for glacial isostatic adjustment studies: the influence of gravitational loading effects on secular gravity trends, *J. Geodyn,* **102,** 83–94.

Pagiatakis, S.D. & Salib, P., 2003. Historical relative gravity observations and the time rate of change of gravity due to postglacial rebound and other tectonic movements in Canada, *J. geophys. Res.,* **108**(B9), 2406, doi:10.1029/2001JB001676.

Pálinkáš, V., Lederer, M., Kostelecký, J., Simek, J., Mojzeš, M. & Csapó, D., 2012. Analysis of the repeated absolute gravity measurements in the Czech Republic, Slovakia and Hungary from the period 1992-2010 considering instrumental and hydrological effects, *J. Geod.,* **87**(1), 29–42.

Pálinkáš, V. *et al.*, 2017. Regional comparison of absolute gravimeters, EURAMET.M.G-K2 key comparison, *Metrologia,* **54**(1A), 07012, doi:10.1088/0026-1394/54/1a/07012.

Peltier, W.R., Argus, D.F. & Drummond, R., 2015. Space geodesy constrains ice-age terminal deglaciation: the global ICE-6G_C (VM5a) model, *J. geophys. Res.,* **120,** 450–487.

Pettersen, B.R., 2011. The postglacial rebound signal of Fennoscandia observed by absolute gravimetry, GPS and tide gauges, *Int. J. Geophys.,* doi:10.1155/2011/957329.

Pettersen, B.R. *et al.*, 2010. An accuracy assessment of absolute gravimetric observations in Fennoscandia, *Nord. J. Surv. Real Estate Res.,* **7**(1), 7–14.

Pitkänen, M.R.A., Mikkonen, S., Lehtinen, K.E.J., Lipponen, A. & Arola, A., 2016. Artificial bias typically neglected in comparisons of uncertain atmospheric data, *Geophys. Res. Lett.,* **43,** 10003–10011.

Purcell, A., Dehecq, A., Tregoning, P., Potter, E.K., McClusky, S.C. & Lambeck, K., 2011. Relationship between glacial isostatic adjustment and gravity perturbations observed by GRACE, *Geophys. Res. Lett.,* **38,** L18305, doi:10.1029/2011GL048624.

Robertsson, L. *et al.*, 2001. Results from the fifth international comparison of absolute gravimeters, ICAG97, *Metrologia,* **38,** 71–78.

Roland, E., 1998. *Absolutt tyngdemåling i fennoskandia ag svalbard,* Internal Project Report (in norwegian), Norwegian Mapping Authority.

Sato, T. *et al.*, 2012. Gravity and uplift rates observed in southeast Alaska and their comparison with GIA model predictions, *J. geophys. Res.,* **117,** B01401, doi:10.1029/2011JB008485.

Steffen, H. & Kaufmann, G., 2005. Glacial isostatic adjustment of Scandinavia and northwestern Europe and the radial viscosity structure of the Earth's mantle, *Geophys. J. Int.,* **163**(2), 801–812.

Steffen, H. & Wu, P., 2011. Glacial isostatic adjustment in Fennoscandia – a review of data and modeling, *J. Geodyn.,* **52,** 169–204.

Steffen, H., Gitlein, O., Denker, H., Müller, J. & Timmen, L., 2009. Present rate of uplift in Fennoscandia from GRACE and absolute gravimetry, *Tectonophysics,* **474,** 69–77.

Steffen, H., Wu, P. & Wang, H., 2012. Optimal locations for absolute gravity measurements and sensitivity of GRACE observations for constraining

glacial isostatic adjustment on the northern hemisphere, *Geophys. J. Int.,* **190,** 1483–1494.
Steffen, H., Wu, P. & Wang, H., 2014. Optimal locations of sea-level indicators in glacial isostatic adjustment investigations, *Solid Earth,* **5,** 511–521.
Steffen, H. *et al.*, 2016. NKG201xGIA a model of glacial isostatic adjustment for Fennoscandia, *Proc. NKG General Assembly,* Göteborg, Sweden, 1–4 September 2014, Lantmäterirapport 2007:4, pp. 85–86, ed. Kempe, C., Lantmäteriet.
Timmen, L., Falk, R., Gitlein, O. & Wilmes, H., 2011. The measuring offset of the absolute gravimeter JILAg-3 (LUH) with respect to the FG5 instruments no. 101(BKG) and no. 220 (LUH), in *Terrestrial Gravimetry: Static and Mobile Measurements, Int. Symposium,* pp. 72–77, ed. Peshekhonov, V.G., The State Research Center of Russian Federation Concern CSRI Elektropribor, JSC.
Timmen, L., Gitlein, O., Klemann, V. & Wolf, D., 2012. Observing gravity change in the Fennoscandian uplift area with the Hanover absolute gravimeter, *Pure appl. Geophys.,* **169,** 1331–1342.
Timmen, L., Engfeldt, A. & Scherneck, H.-G., 2015. Observed secular gravity trend at Onsala station with the FG5 gravimeter from Hannover, *J. Geod. Sci.,* **5,** 18–25.
Torge, W., Röder, R.H., Schnüll, M., Wenzel, H.-G. & Faller, J.E., 1987. First results with the transportable absolute gravity meter JILAG-3, *Bull. géodésique,* **61**(2), 161–176.
Torge, W., Falk, R., Franke, A., Reinhart, E., Richter, B., Sommer, M. & Wilmes, H., 1999. *Das Deutsche Schweregrundnetz 1994 (DSGN94),* DGK B309, Munich.
Van Camp, M., Williams, S.D.P. & Francis, O., 2005. Uncertainty of absolute gravity measurements, *J. geophys. Res.,* **110**(B05406), doi:10.1029/2004JB003497.
Van Camp, M., Meurers, B., de Viron, O. & Forbriger, T., 2016a. Optimized strategy for the calibration of superconducting gravimeters at the one per mille level, *J. Geod.,* **90,** 91–99.
Van Camp, M., Viron, O. & Avouac, J.P., 2016b. Separating climate-induced mass transfers and instrumental effects from tectonic signal in repeated absolute gravity measurements, *Geophys. Res. Lett.,* **43**(9), 4313–4320.
Van Camp, M., de Viron, O., Watlet, A., Meurers, B., Francis, O. & Caudron, C., 2017. Geophysics from terrestrial time-variable gravity measurements, *Rev. Geophys.,* **55,** 4, 938–992.
van Dam, T., Francis, O., Wahr, J., Khan, S.A., Bevis, M. & van den Broeke, M.R., 2017. Using GPS and absolute gravity observations to separate the effects of present-day and Pleistocene ice-mass changes in South East Greenland, *Earth planet. Sci. Lett.,* **459,** 127–135.
Vestøl, O., 2007. Determination of postglacial land uplift in Fennoscandia from leveling, tide-gauges and continuous GPS stations using least squares collocation, *J. Geod.,* **80,** 248–258.
Virtanen, H., 2006. *Studies of Earth Dynamics with the Superconducting Gravimeter,* PhD thesis, University of Helsinki.
Virtanen, H., Bilker-Koivula, M., Mäkinen, J., Näränen, J., Raja-Halli, A. & Ruotsalainen, H., 2014. Comparison between measurements with the superconducting gravimeter T020 and the absolute gravimeter FG5-221 at Metsähovi, Finland in 2003-2012, *Bull. Inf. Marées Terrestres,* **148,** 11923–11928
Vitushkin, L. *et al.*, 2002. Results of the sixth international comparison of absolute gravimeters, ICAG-2001, *Metrologia,* **39,** 407–424.
Wahr, J., DaZhong, H. & Trupin, A., 1995. Predictions of vertical uplift caused by changing polar ice volumes on a viscoelastic earth, *Geophys. Res. Lett.,* **22**(8), 977–980.
Wilmes, H., Richter, B. & Falk, R., 2003. Absolute gravity measurements: a system by itself, in *Proc. 3rd Meeting of the International Gravity and Geoid Commission: Gravity and Geoid 2002,* pp. 19–25, ed. Tziavos, I.N., IAG, Ziti Editions, Thessaloniki, Greece.
Wu, P. & Peltier, W.R., 1982. Viscous gravitational relaxation, *Geophys. J. R. astr. Soc.,* **70,** 435–485.

## SUPPORTING INFORMATION

Supplementary data are available at *GJI* online.

**Table S1.** Providers of the data in Tables S2 and S4.
**Table S2.** Absolute gravity stations in Fennoscandia. VGG is the vertical gravity gradient 1.2 m above the floor, $n_{obs}$ the number of absolute gravity observations and $\Delta T$ the time span between first and last observation.
**Table S3.** Parameters used to reduce JILAg observations on Estonian stations to reference height 1.20 m.
**Table S4.** Complete list of observations. $\sigma_{set}$ is the set scatter, i.e. the standard deviation of the set values, and $\sigma_{tot}$ is the total uncertainty taken into account also the uncertainty from possible instrumental systematic effects or biases (Niebauer *et al.* 1995). JOEN, SODA, VAAA, VAAB observations are at 1.00 m reference height (approximately mean observation height for stations with both JILAg and FG5 observations), the rest at 1.20 m. Different reference heights at different stations only affect the absolute gravity values and not estimates of $\dot{g}$. NaN means that data were not available for the authors.

Please note: Oxford University Press is not responsible for the content or functionality of any supporting materials supplied by the authors. Any queries (other than missing material) should be directed to the corresponding author for the paper.